Characterization of Cyanophages on Cyanobacteria for Potential Control of Harmful Algal Blooms

Undergraduate Honors Thesis

Presented in Partial Fulfillment of the Requirements for

Graduation with Distinction in the

Department of Mechanical Engineering at

The Ohio State University

Chanhee John Ha

Undergraduate Program in Mechanical Engineering

The Ohio State University

2017

Advisor: Hanna Cho, Ph.D.

Abstract

Cyanobacteria are responsible for the toxins produced by Harmful Algal Blooms (HABs) that pose extremely hazardous environmental risks to humans, wildlife and the ecosystem. Cyanophages act as viruses on host cyanobacteria and can deter or improve their growth through lysis or lysogenesis, depending on the factors the cyanophages carry; in turn, affecting the growth of HABs (Watkins, 2014). Whereas this general cyanophage-cyanobacteria relationship is understood, freshwater cyanobacteria has been less studied in comparison to its saltwater counterpart. These freshwater cyanobacteria must be studied as they remain prominent problems to clean drinking water and inland agriculture. Little information on detailed characteristics of this relationship, such as morphological and mechanical property change over time, exists. In this work, Atomic Force Microscopy (AFM) was employed to characterize the lytic relationship between cyanobacteria *Microcystis aeruginosa* and cyanophage Ma-LEP. Results from AFM show degradation of the cyanobacteria (decrease in height, Young's modulus) over a 1 month period, showing signs of lysis within 6 hours of being introduced to cyanophage. This is the first study (to our knowledge) to mechanically define this relationship. Characterization of the lytic behavior of Ma-LEP when encountering *Microcystis aeruginosa* proves useful as defining a specific time of lytic behavior and rate of degradation of the bacteria is essential in using cyanophages as a biocontrol for HABs.

Acknowledgements

First, I would like to thank my advisor, Professor Hanna Cho. In December of 2016, I made the decision to go to graduate school. I made the decision to apply for the Mechanical Engineering undergraduate research program extremely late and on a whim. Despite not knowing Dr. Cho, she accepted me in her lab almost instantly with the little credentials I had, gave me a project to work on with minimal experience, and continued to advise me despite my constant shortcomings. Any time in the future where I look back on my career, that gesture will always be something my future was dependent on, and for that, I am eternally grateful.

For the same reasons, I would also like to thank the Micro/Nano Multiphysical Dynamics Lab, Jinha Kwon in particular, for being constant mentors to me. Thank you for putting up with my inexperience and taking time out of your busy schedules to teach me.

Third, I would like to thank Professor Jiyoung Lee, Xuewen Jiang, and Seungjun Lee for their continual help and tutelage on the subject of my thesis. Thank you for your quick responses, as this thesis would not have been possible without them. Their help has given me a new perspective on environmental studies and will be an interest of mine moving forward.

Thrid, I would like to thank Professor Satya Seetharaman for being a life coach outside of our teacher-grader relationship of the past three years. He directed me to Dr. Cho as I had previous lab experience with Atomic Force Microscopy. The memorable style of teaching and book exchanging is something I will remember as I leave undergraduate college and is something I hope to do with students if I teach in the future.

I would like to thank Professor Siston for accepting me to the undergraduate research program despite being over a month tardy to the research proposal deadline. Thank you for constantly challenging me to push my brain and personality to develop as an engineer.

Last and not least, my friends and family have served as a personal anchor throughout my long tenure here in undergraduate college. I have always overthought important decisions – major, jobs, research focus. Numerous people have helped me with important decisions that shaped the future I want. I will do better in decision making in the future.

Table of Contents

List of Figures

List of Tables

List of Appendix Figures

Chapter 1: Introduction

1.1 Harmful Algal Blooms (Macroscale)

As the need for clean water becomes more urgent by the minute, the removal of pollution from freshwater has become increasingly necessary. Issues such as the recent Flint, MI water crisis of 2016 are still completely unresolved due to improper water quality standards [1]. Large scale freshwater problems such as these can be resolved by providing a different water source, such as the Great Lakes. The Great Lakes currently supply 84% of North America's surface fresh water and about 21% of the world's supply of surface fresh water [2]. However, large bodies of freshwater, such as Great Lakes, have also been polluted naturally through Harmful Algal Blooms (HABs).

The United States Environmental Protection Agency (EPA) classifies HABs as overgrowths of algae in water that pollute the water in two ways:

(i) Growing uncontrollably and their sheer biomass populates the lake, and/or

(ii) Through the production of toxins.

HABs grow out of control when in a slow-moving body of water and exposed to sunlight and excessive nutrients such as nitrogen and phosphorus. Figure 1 shows the scale of freshwater Harmful Algal Blooms in the Great Lakes when exposed to these factors.

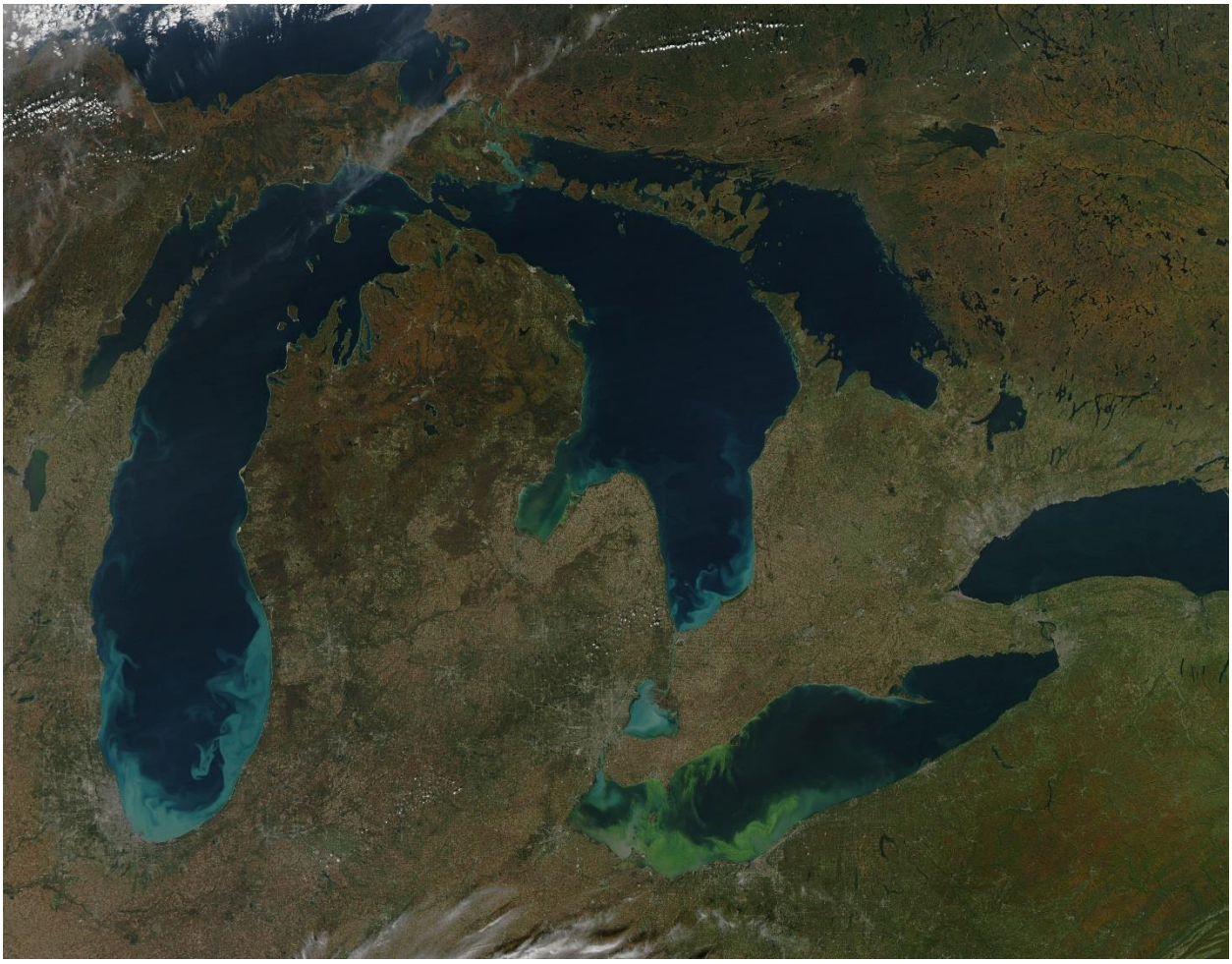

Figure 1: Aerial View of the Great Lakes (Dark Blue) with Harmful Algal Blooms (Blue-Green) during Summer of 2011. *[3]*

In environments such as the Great Lakes seen in Fig. 1, the surrounding agriculture causes the water to become eutrophic. The native algae feed off the nutrient rich water and grow uncontrollably [2]. These toxins kill the native wildlife and are also extremely toxic to humans, such as neurotoxins, hepatotoxins, and dermatoxins, creating dead zones in the water [4] [5]. Such toxin pollution has affected states such as Ohio, where a summer resurgence of HABs in Lake Erie caused a three-day tap water ban of Toledo, Ohio in 2014 [6]. Other downstream effects of freshwater HABs such as water deoxygenation and water supplies can be seen in the diagram of Fig. 2.

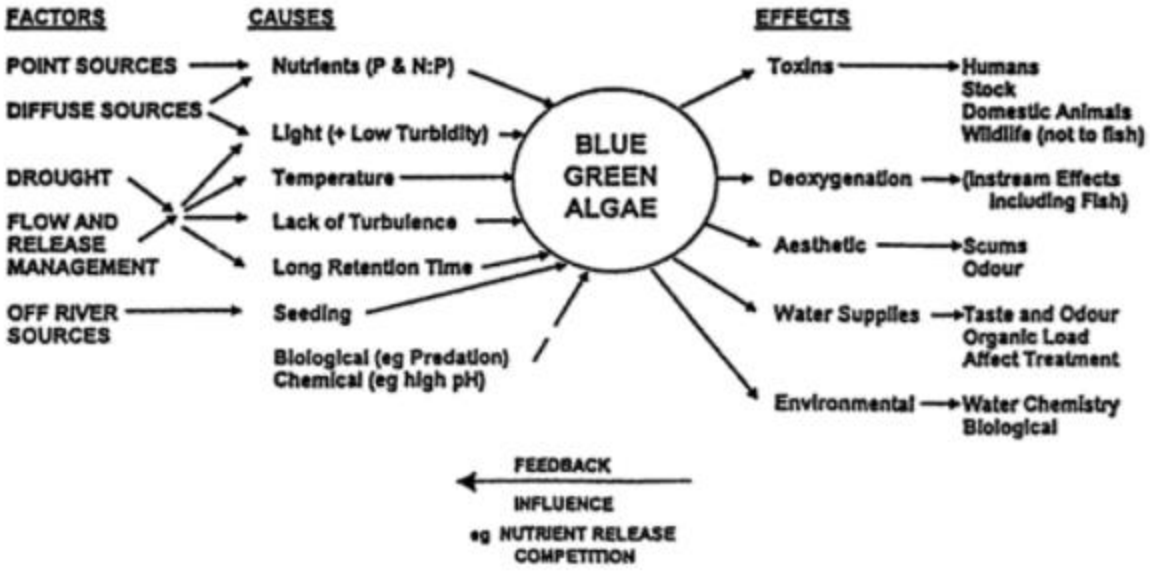

Figure 2: Factors, Causes, and Effects of Freshwater Harmful Algal Blooms *[7]*

HABs also cause economic loss. Research of saltwater HABs is driven by the shellfish industry suffering from toxins emitted by HABs. Humans contracting diseases from consuming poisoned toxins, such as amnesic shellfish poisoning call for heavy monitoring of the coastal regions of the United States [8]. A 2002 study by the Woods Hole Oceanographic Institution estimated the total cost of monitoring HABs in 11 states with high algae populations at around 2 million dollars. For the southwest coast of Florida alone, the cost of beach cleanups surmounted 170 thousand dollars per year [9]. The large economic effects of saltwater HABs have caused saltwater HABs to be more heavily studied. In the same context, it is economically urgent to mitigate the problems caused by freshwater HABs.

1.2 Harmful Algal Blooms (Microscale)

The primary suspect of freshwater HAB toxin formation is cyanobacteria. Cyanobacteria are photosynthetic prokaryotes – the root word “cyan” in cyanobacteria refers to their ability to

synthesize chlorophyll-a, giving the HABs their blue-green color seen in Fig. 1 [10]. When the cyanobacteria are exposed to eutrophic water, they have the ability to form secondary metabolites, or the toxins listed in the previous section [11]. In the Great Lakes, the most prevalent toxin-producing cyanobacteria is *Microcystis.* In humans, *Microcystis* is known to produce hepatotoxins causing liver failure, ultimately leading to heart failure and death. The ecotoxicology of *Microcystis* has been known to fatally affect farm and lake wildlife including cattle, sheep, pigs, and fish, promoting tumor growth and poisoning [11] [12] [13].

1.3 Biological Pathways

To deter the growth of cyanobacteria, cyanophage has been introduced. A cyanophage is a virus that infects specifically cyanobacteria. There are two possibilities when introducing a cyanophage to cyanobacteria:

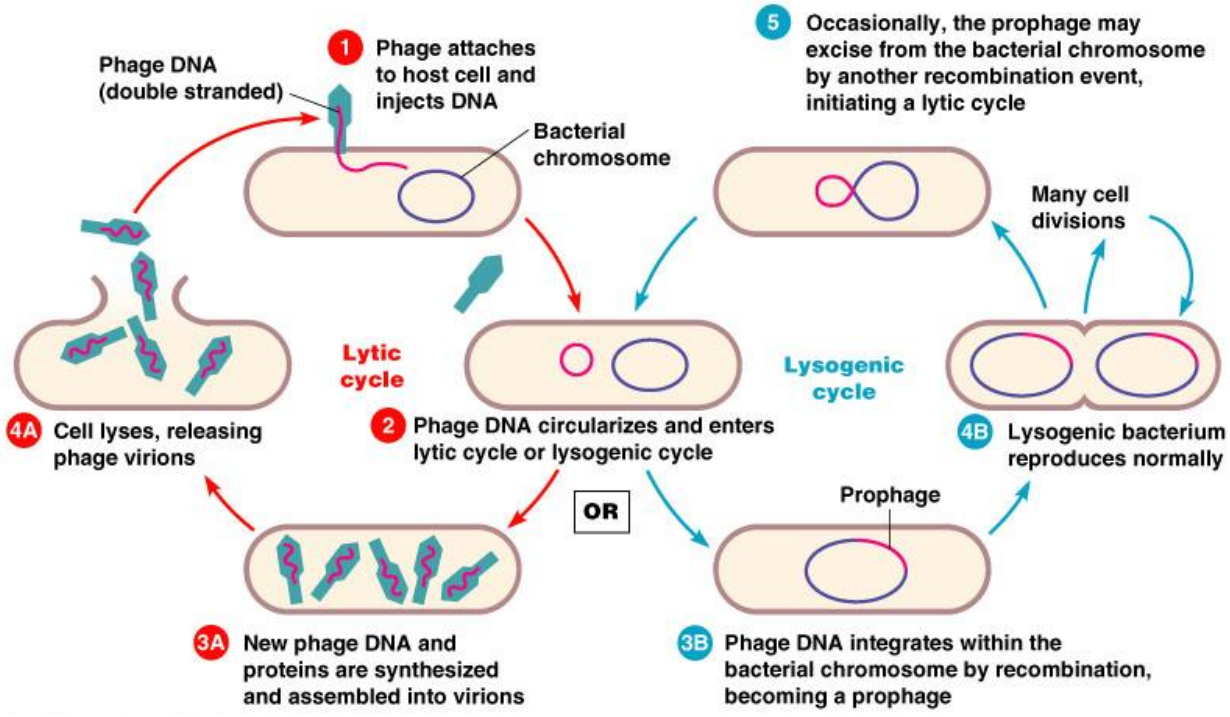

Figure 3: Lysis (left) and lysogenesis (right) of cyanophage and cyanobacteria *[14]*.

(i) Lysis, where the cyanophage infects the cyanobacteria and replicates itself within the cyanobacterial cell walls. The cell ruptures, or lyses, releasing copies of the cyanophage.

(ii) Lysogenesis, where the cyanophage infects the cyanobacteria and incorporates its DNA with the cyanophage's DNA. As the cell replicates, the cyanophage's DNA is passed on and is also replicated.

In a larger scale, lysis would collapse the population by causing eventual degradation of the cyanobacterial population. Lysogenesis would influence genetic diversity and strain succession [15]. To attack and degrade a cyanobacteria population such as *Microcystis* in the Great Lakes, the lytic cycle would need to be utilized. To trigger the lytic cycle, chemical or physical agents such as mitomycin C or UV light are used at the crossroad Step 2 in Fig. 3. By triggering lysis throughout the *Microcystis* population in the Great Lakes, a decrease in toxin production would lead to an overall cleaner ecosystem for humans and wildlife to use [15].

Though the general characteristics of the lytic relationship between cyanobacteria and cyanophages is understood due to studies on saltwater cyanobacteria, characteristics of this relationship are poorly understood for freshwater bacteria. Such characteristics include the time of lysis, the rate of degradation, and the rate of stiffness change in the bacteria. These must be distinguished in order to properly utilize the lytic cycle as an eventual biocontrol for the *Microcystis* population, and in turn, providing a cleaner ecosystem.

1.4 Objectives

Studying the various properties of the lytic interaction between cyanobacteria and cyanophage would be the first of its kind and would be extremely valuable to developing a biocontrol for freshwater HABs.

This experiment has several objectives:

(i) Physically characterize the lytic cyanobacteria-cyanophage cycle by observing morphological change over time.

(ii) Mechanistically characterize the lytic cyanobacteria-cyanophage cycle by measuring stiffness change over time.

(iii) Observe chemical composition changes in the lytic cyanobacteria-cyanophage cycle.

(iv) Discover the rate of the lytic cyanobacteria-cyanophage cycle via *in-situ* measurement.

Chapter 2: Characterization of Lytic Cycle with Atomic Force Microscopy

2.1 Current Characterization Methods of Lytic Cycle Measurement

The most commonly used methods in cyanobacterial characterization are Scanning Electron Microscopy (SEM) and Transmission Electron Microscopy (TEM). SEM functions by scanning the surface with a beam of electrons, measuring the change in electron interactions with the surface to give information on the cyanobacteria's morphology and topography. TEM functions by transmitting a beam of electrons through a thin section of the sample, which is then

magnified and project onto a fluorescent screen. The advantages of these modes include high resolution of images with quick scanning times close to real-time.

However, there are a few drawbacks to these modes, especially in biological applications. As these two methods function using electrons, a high vacuum is required to operate. In addition, sample preparation requires the cyanobacteria to be killed and coated with conductive material such as gold in order to interact with electrons. This type of sample preparation makes it impossible to perform in-situ measurements and accurately find a rate or time of lysis.

Second, due to the utilization of electron interaction rather than "feeling" the surface, it is impossible to find mechanical characteristics, such as Young's Modulus, of the cyanobacteria. SEM is often used to find changes in topography but outputs as an image – it may be possible to find some dimensions of the cyanobacteria, but measuring height is almost unachievable due to the low amount of contrast and obscuring of collateral surface features. TEM is often used to show the sample in its entirety, but the output of TEM is a two-dimensional image, again giving an inaccurate representation of the actual cyanobacteria [16].

2.2 Use of Atomic Force Microscopy

The use of Atomic Force Microscopy (AFM) is increasingly popular as its capabilities are very compatible with biological applications. In bacterial studies, the different modes of AFM give high resolution, 3D images of the bacteria. AFM provides a "sense of touch" as a microcantilever tip "feels" the surface of the sample, also giving information on mechanical properties. In addition, the use of AFM allows for in-situ study in air or liquid while keeping the sample intact or even alive. This also allows the user to observe mechanical properties of the cyanobacteria in its own lake environment and even view the cyanobacteria-cyanophage interaction in-situ.

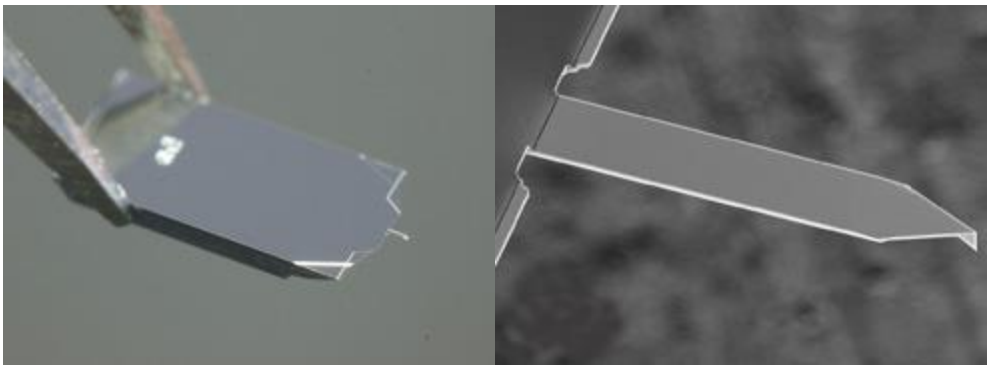

Figure 4: AFM Microcantilever (Left) with Probe Tip (Right) *[17]*

2.3 Atomic Force Microscopy Function

AFM functions by probing the deflection of a microcantilever with a small tip scanning along the surface of the sample. A laser reflecting off of the back of the cantilever is directed into a four-quadrant photodiode to monitor the deflection of the microcantilever in response to the tip-sample interactions.

There are three categories of AFM operational mode distinguished by how the tip interact with the sample: contact, non-contact, and tapping mode. Contact mode drags the cantilever tip over the surface, copying the surface topography as it moves. However, contact mode in biological applications such as cyanobacteria is often avoided due to the softer nature of the sample. In non-contact mode, the cantilever oscillates above but close to the sample. The tip interacts with van der Waals forces to change the resonance frequency of the microcantilever. However, this mode generally provides a lower resolution of image and contaminants on the surface may affect the actual topography of the surface.

Tapping mode of AFM was used throughout the entirety of this experiment due to its advantages and ability to avoid the issues listed above. The cantilever taps along the surface of

the sample, its primary advantages being minimal damage to the tip and sample surface due to minimized tip-sample interaction. [18].

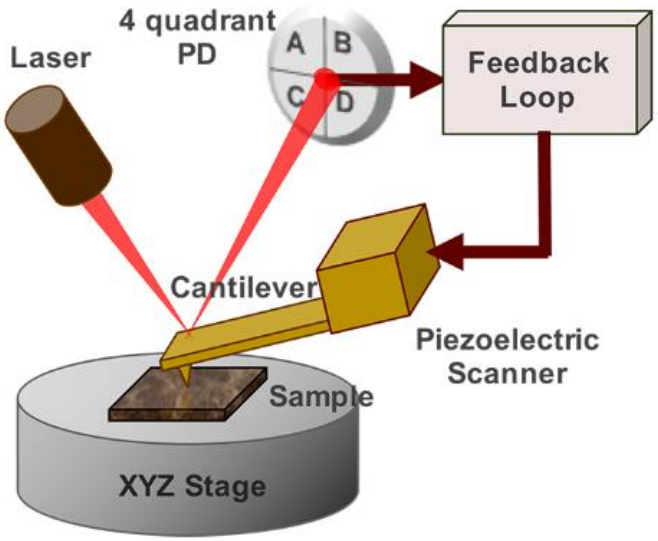

Figure 5: Visualization of AFM Feedback Loop

2.2.1 AC Air Tapping Mode

AC Air Tapping Mode of AFM functions by oscillating the cantilever near its resonance frequency. When scanning the surface of the sample, the AFM outputs three main images: Height, Amplitude, and Phase. The Height image serves as a topographic map of the surface. Varying heights on the sample surface cause the oscillating cantilever to deflect. Through the AFM's feedback loop, the cantilever height is held constant to achieve a constant laser position. Doing so provides an accurate map of the height changes along the sample. The Amplitude image measures changes in the input drive signal of the cantilever tip as it runs along the surface of the cantilever. These deflections are measured by the four-quadrant photodiode and are read as a DC signal by the AFM's feedback loop. The DC signal is translated into topographic information experienced by the deflection of the cantilever. Lastly, Phase imaging measures the

phase lag between the input drive signal from the piezoelectric driver and the output oscillation signal. Varying phase lags correspond to energy dissipation from varying material stiffness properties on the sample surface. This lag is simultaneously recorded with topographic change in the sample so the corresponding material stiffness changes are mapped with their respective topographic changes [19]. Differences in material stiffness are distinguished on the phase image by viewing "attractive" and "repulsive" regions. A cantilever enters an attractive region when either experiencing van der Waals forces between the tip and the sample and when indenting a material. When the cantilever can no longer indent the material, the cantilever enters the repulsive region. This indicates that the cantilever is now experiencing a deflection due to the stiffness of the sample. As a result, materials with a lower stiffness will indent more, causing a larger phase lag and a phase reading of over 90 degrees. In contrast, materials with higher stiffness will cause the cantilever to deflect instead, resulting in a lower phase lag and a phase reading of under 90 degrees. This mode was selected to view height and material stiffness changes during degradation of the cyanobacteria.

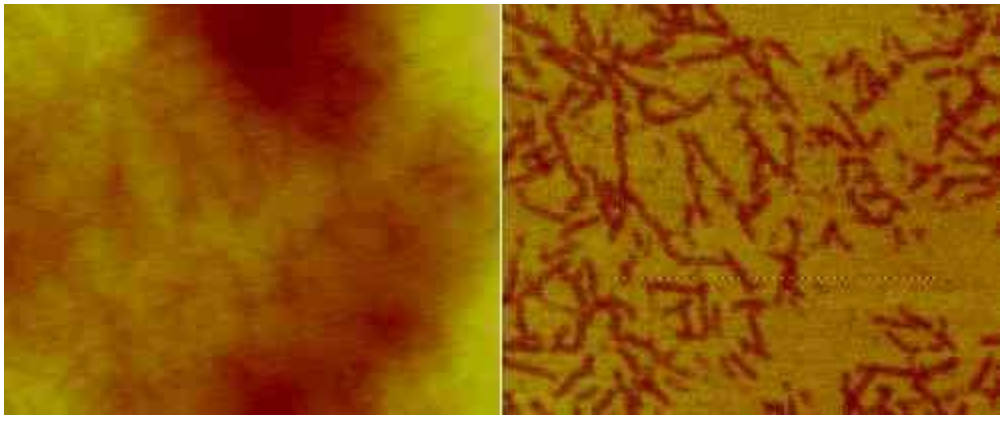

Figure 6: AC Air Tapping mode of copolymer surface. Phase image (right) reveals material property differences not seen in Height image (left). Red regions on the Phase image indicate repulsive regions, or regions with higher material stiffness, causing less of a phase lag and a lower phase reading. Yellow regions in the Phase image indicate more attractive regions with lower material stiffness, causing a greater phase lag and higher phase reading *[20]*.

2.2.2 AM-FM Viscoelastic Mapping Mode

AM-FM, or Amplitude Modulation – Frequency Modulation, functions similarly to AC Air Tapping Mode. In AC Air Tapping Mode, one mode is excited to give topographic information. AM-FM Viscoelastic Tapping Mode functions as a bimodal AFM by simultaneously exciting two resonant frequencies, one high and one low, into the microcantilever to discover additional information on the sample. The AM frequency, or the low frequency, functions in standard tapping mode, and changes in this mode correspond to topography, similar to AC Air Tapping Mode mentioned before. The higher, unperturbed FM frequency "rides along" the AM frequency. Changes in this higher frequency correspond to changes in stiffness and elasticity [21]. This mode was chosen to reveal a changes in Young's Modulus along the cyanobacteria surface at different times during the lytic cycle.

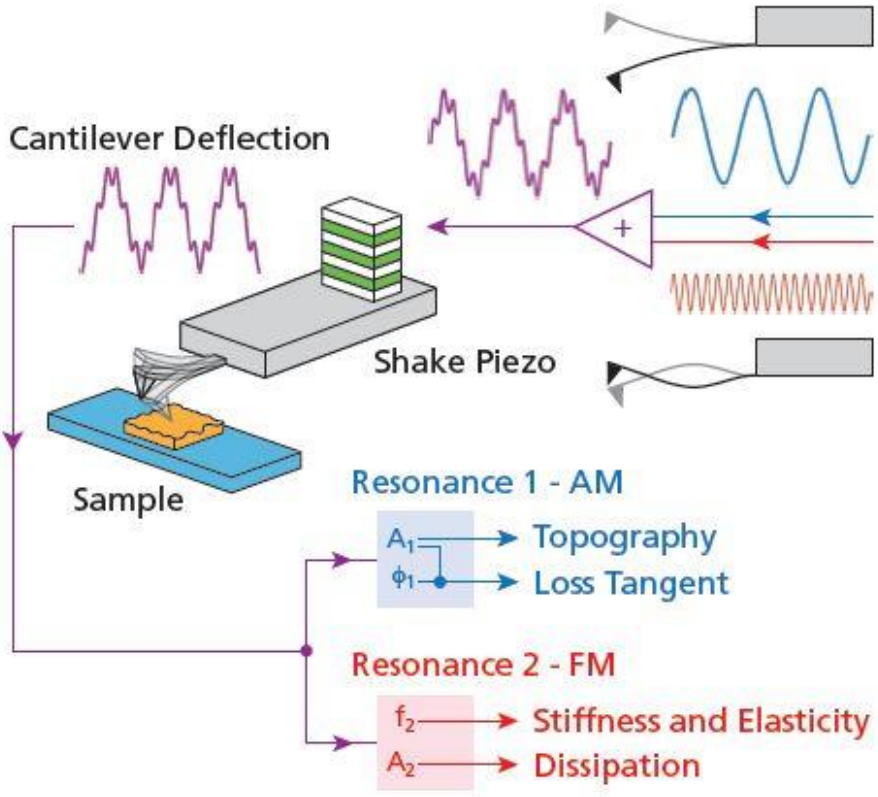

Figure 7: Schematic of AM-FM Viscoelastic Mapping Mode Function with AM and FM frequency inputs and topography and stiffness outputs *[21]*.

2.2.3 AFM-IR Spectroscopy

In normal practice, IR Spectroscopy involves pulsing infrared radiation at a certain molecular compound. Doing so causes the intermolecular bonds of the compound to vibrate at their resonant frequencies. As a result, IR Spectroscopy is useful to find the molecular structure of a compound due to its ability to distinguish different molecular bonds within a compound. AFM – Infrared Spectroscopy combines this principle with AFM by pulsing infrared radiation at the tip of the AFM cantilever. The resulting excitation amplitude of the oscillation is proportional to the sample properties. Depending on the chemical composition of the sample under the AFM tip, the cantilever will undergo excitation differently. The output of this mode, similar to normal IR Spectroscopy, is an absorption spectrum that is unique to every chemical compound. The purpose of AFM-IR in this experiment is to reveal different chemical changes that *Microcystis aeruginosa* could be undergoing during the lytic cycle. In addition, it is to chemically confirm evidence of cyanophage on or around the cyanobacteria during the lytic cycle [22].

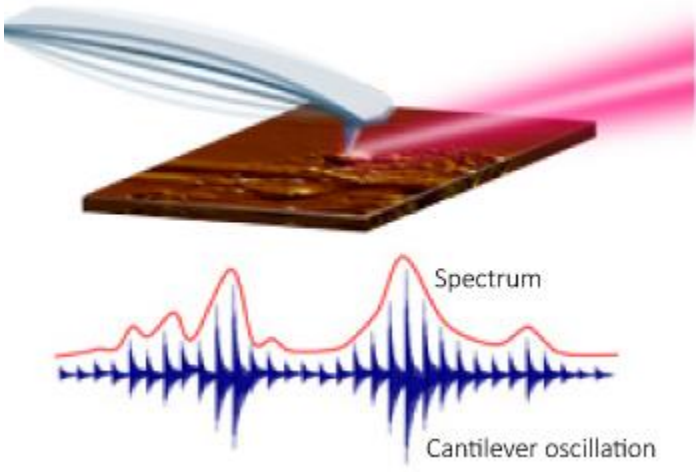

Figure 8: Schematic of infrared excitation of tip and sample producing spectrum *[22]*.

2.2.4 Liquid AFM Mode

Liquid AFM Mode functions the same as AC Air Tapping Mode, but within in a liquid cell. The outputs of Liquid AFM are also the same as AC Air Tapping Mode: Height, Amplitude, and Phase images.There are several benefits of using liquid over air AFM measurements. The ability to use lake water for the cyanobacteria *in-situ* provides a more accurate representation of the cyanobacteria's actual environment [18]. In addition, this mode is being used in order to view a live interaction of the lytic cycle over time through continuous scanning of the cyanobacteria-cyanophage interaction over several hours. The use of a fluid cell also makes injection of the phage into the lake water during scanning feasible. As a result, these advantages give Liquid AFM Mode a more accurate, *in-situ* advantage.

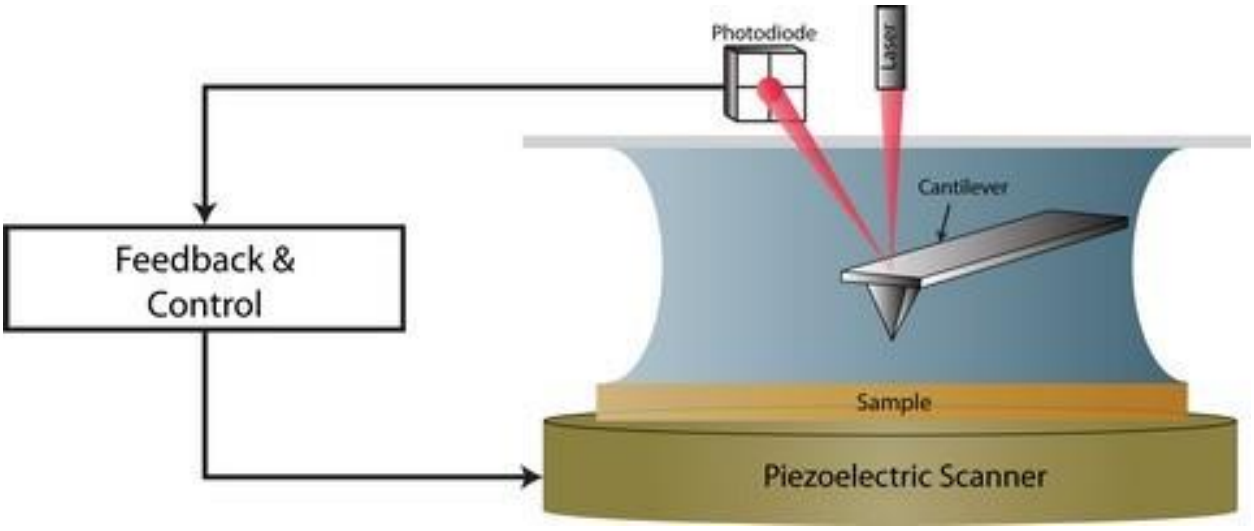

Figure 9: Schematic of Liquid AFM feedback loop with submerged cantilever *[23]*.

Chapter 3: Materials and Methods

3.1 Sample Preparation

3.1.1 Selection of Cyanobacteria

Previous studies by The Ohio State University Department of Food Science and Technology showed cyanophages potentially affecting populations of toxic *Microcystis*

aeruginosa. Samples of *Microcystis aeruginosa* was collected in water samples from Lake Erie from 2013 to 2015, then were isolated and cultured [24].

3.1.2 Selection of Cyanophage

Water samples with cyanophage were collected from Lake Erie in the summer from 2013 to 2015, then concentrated by Centripep® Centrifugal Filters YM-50 by The Ohio State University Department of Food Science and Technology. 22 different cyanophages were screened by adding 50 µl of cyanophage concentrate to 100 µl of *Microcystis aeruginosa culture* and incubated at room temperature with a 12 hour light cycle for two days. The phage selected for AFM analysis, cyanophage Ma-LEP, showed lytic activity [24] [25].

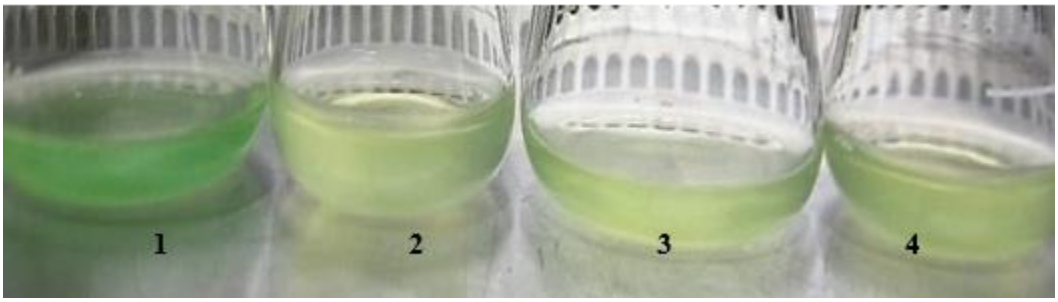

Figure 10: The impact of cyanophages on the growth of M. aeruginosa culture when different amount of cyanophages were added (1: without cyanophages; 2 and 3: with 5ml of cyanophages; 4: with 1ml of cyanophages) *[24]*.

3.1.3 AFM Sample Preparation

For AC Air Tapping and AM-FM Viscoelastic Tapping Modes, 1x1 cm squares of mica were freshly cleaved and dipped in gelatin solution (.5 grams gelatin per 100 mL deionized water) at 60-70°C (Sigma, CAS #9000-70-8, St. Louis, MO, USA; p/n 56-75, Highest Grade Mica Sheet, Ted Pella Inc., Redding, CA, USA). After 24 hours of drying, 10 µL of *Microcystis*

aeruginosa culture was aliquoted onto the gelatin-coated mica, rested for 10 minutes, washed with deionized water to remove excess propagation material, and left to dry at room temperature [26].

For AFM-IR and Liquid AFM, mica was cut to the size of a correlative microscopy coverslip (Electron Microscopy Sciences, Hatfield, PA, USA) to provide a 1x1 cm reference grid. The same gelatin-coating procedure was used for the mica, which was then mounted onto the coverslip using epoxy glue. The same aliquoting procedure was also used to mount the sample on the mica.

The following samples were prepared for each mode:

Table 1: Sample preparation for each AFM mode.

AC Air Tapping Mode	**AM-FM Viscoelastic Mapping Mode**
1. *Microcystis aeruginosa* (control) 2. 6 hour incubation of *Microcystis aeruginosa* with Ma-LEP 3. 4 day incubation of *Microcystis aeruginosa* with Ma-LEP 4. 1 month incubation of *Microcystis aeruginosa* with Ma-LEP	1. *Microcystis aeruginosa* (control) 2. 6 hour incubation of *Microcystis aeruginosa* with Ma-LEP 3. 1 month incubation of *Microcystis aeruginosa* with Ma-LEP
AFM-IR Spectroscopy	**Liquid AFM**
1. *Microcystis aeruginosa* (control) 2. 2 week incubation of *Microcystis aeruginosa* with Ma-LEP 3. Ma-LEP isolate	1. *Microcystis aeruginosa* (control)

Each sample was mounted onto an AFM Specimen Disc (p/n 16218, Ted Pella Inc., Redding, CA, USA) to remain stationary during scanning.

3.2 Imaging Procedure

All modes of AFM excluding AFM-IR Spectroscopy were performed using MFP-3D Infinity AFM from Asylum Research.

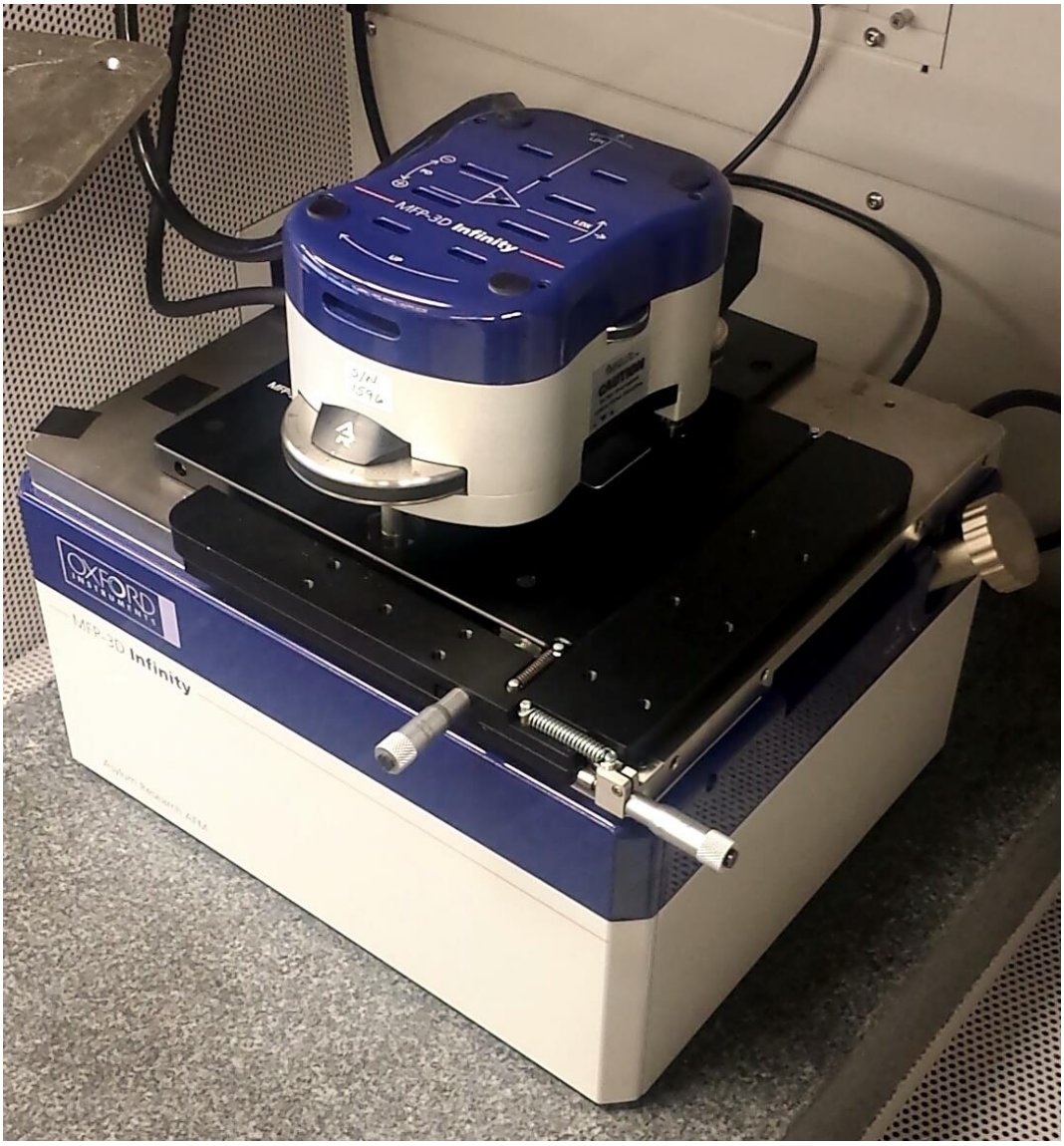

Figure 11: MFP-3D Infinity AFM (Asylum Research)

3.2.1 AC Air Tapping Mode

Imaging in AC Air Tapping mode was performed using a 3D Standard Cantilever Holder (p/n 908.042, Asylum Research, Gotela, CA, USA) equipped with an Olympus® AC240TS Microcantilever (resonant Frequency 70 kHz, Spring Constant 1.7 N/m). Larger images of 20x20 µm were taken at a scan rate of 1 Hz and gain of 20. Smaller images, ranging from 5x5 µm to 10x10 µm, were taken at a scan rate of .5 Hz and gain of 10-15.

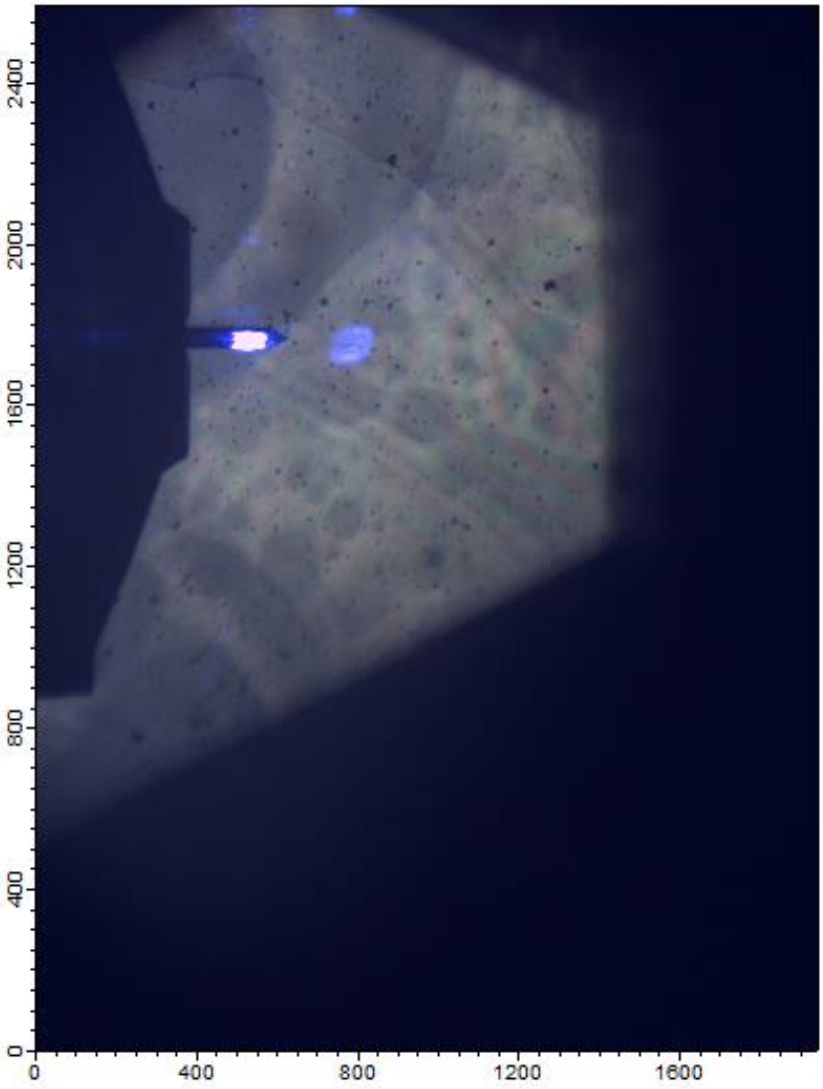

Figure 12: AFM Head Camera view of microcantilever on *M. aeruginosa* (control) surface.

3.2.2 AM-FM Viscoelastic Mapping Mode

Imaging in AM-FM Viscoelastic Tapping mode was performed using a 3D AMFM Cantilever Holder (p/n 908.062, Asylum Research, Gotela, CA, USA) equipped with an Olympus® AC240TS Microcantilever (resonant Frequency 70 kHz, Spring Constant 1.7 N/m). Images ranging from 5x5 µm to 10x10 µm were taken at a scan rate of .5 Hz and gain of 10-15.

3.2.3 AFM-IR Spectroscopy

AC Air Tapping Mode was initially performed on the samples to find desirable locations for AFM-IR Spectroscopy. The following locations were specified on each sample using the reference grid and sent to ANASYS Instruments for AFM-IR Spectroscopy:

Table 2: Specified Reference Grid Rows and Columns for AFM-IR Spectroscopy

Sample	Reference Grid Row	Reference Grid Column
Microcystis aeruginosa (control)	L	10
2 week incubation of *Microcystis aeruginosa* with Ma-LEP	K	11
Ma-LEP isolate	L	10

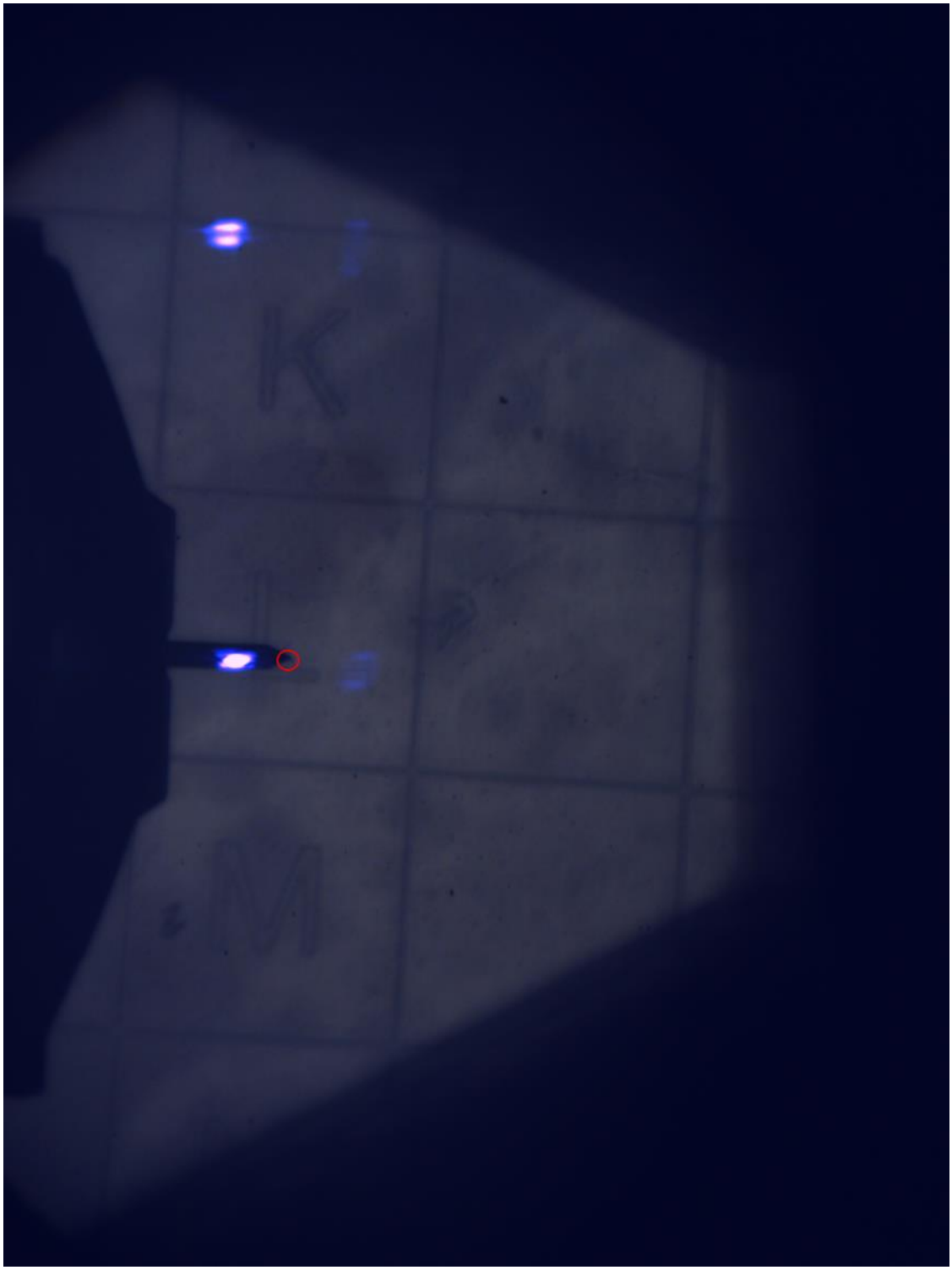

Figure 13: AFM Camera Head View of AFM-IR Spectroscopy Location on Reference Grid (Circled in Red)

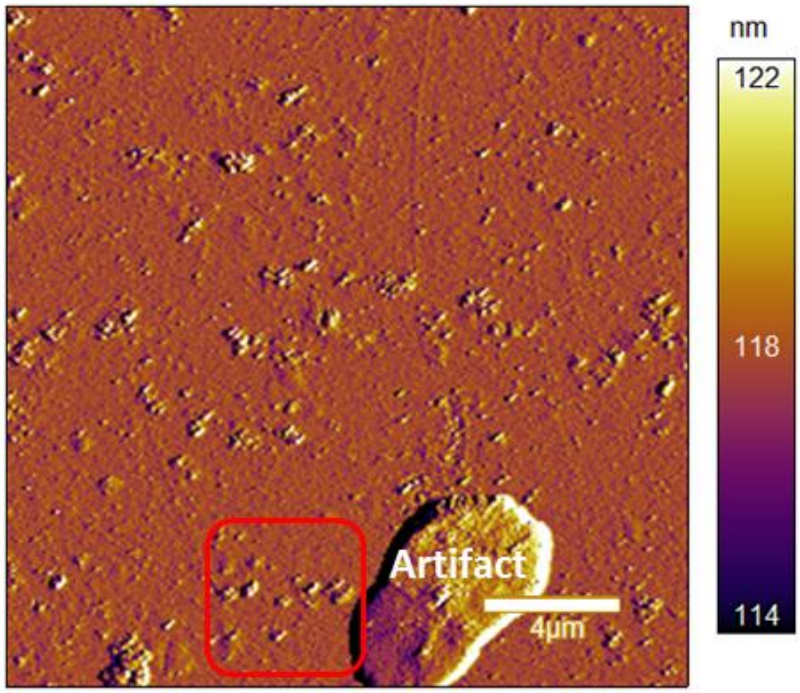

Figure 14: Location of potential Ma-LEP phage pattern (outlined in red) selected for AFM-IR Spectroscopy using AC Air Tapping mode, 20x20 um. This location was chosen due to the nearby artifact used as a landmark.

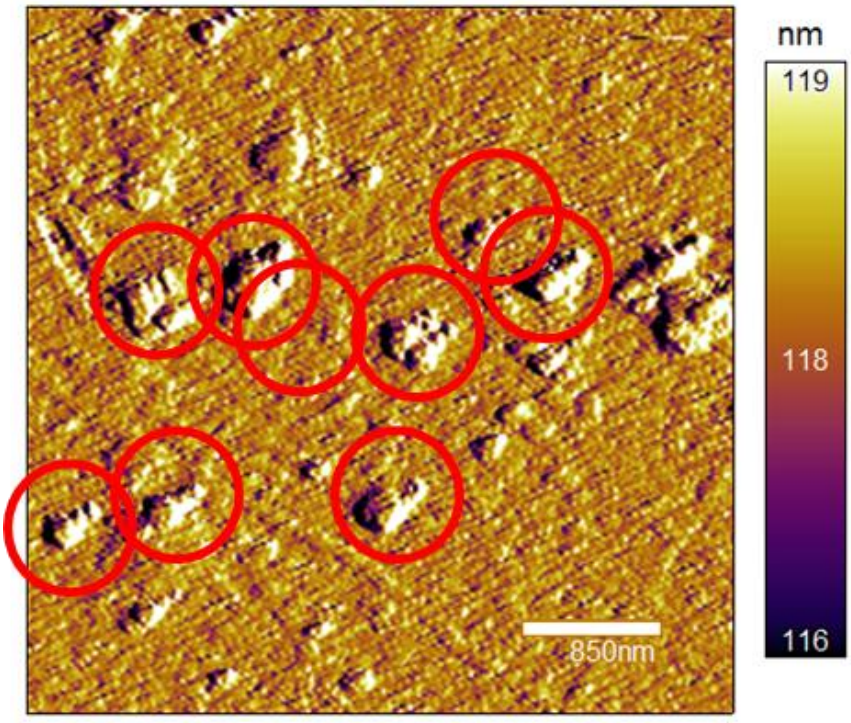

Figure 15: Individual Potential Ma-LEP cyanophages (outlined in red) selected for AFM-IR Spectroscopy using AC Air Tapping Mode, 5x5 um.

3.2.4 Liquid AFM

Lake medium simulating pH and chemical composition of Lake Erie was made and provided by the Department of Food Science and Health for Liquid AFM. Imaging in AC Air Tapping mode was performed using the same cantilever holder and microcantilever as AC Air Tapping Mode. The sample was submerged in the lake medium inside a Closed-Fluid Cell Lite (p/n 900.166, Asylum Research, Gotela, CA). After selecting one control bacteria to scan, Ma-LEP concentrate was injected into the medium via pipette and the same bacteria was repeatedly scanned for 6 hours. Images ranging from 5x5 µm to 20x20 µm in size were taken at a scan rate of .2 Hz and gain of 20.

Figure 16: Asylum Research Fluid Cell Lite with mounted sample submerged in lake medium.

Figure 17: Method of medium and phage injection during in-situ measurement of control sample.

Chapter 4: Results and Discussion

4.1 AC Air Tapping Mode

Scans of 5-10 areas were performed on each time sample to find a representative sample for the population. Figure 17 shows the representative samples at each sample time.

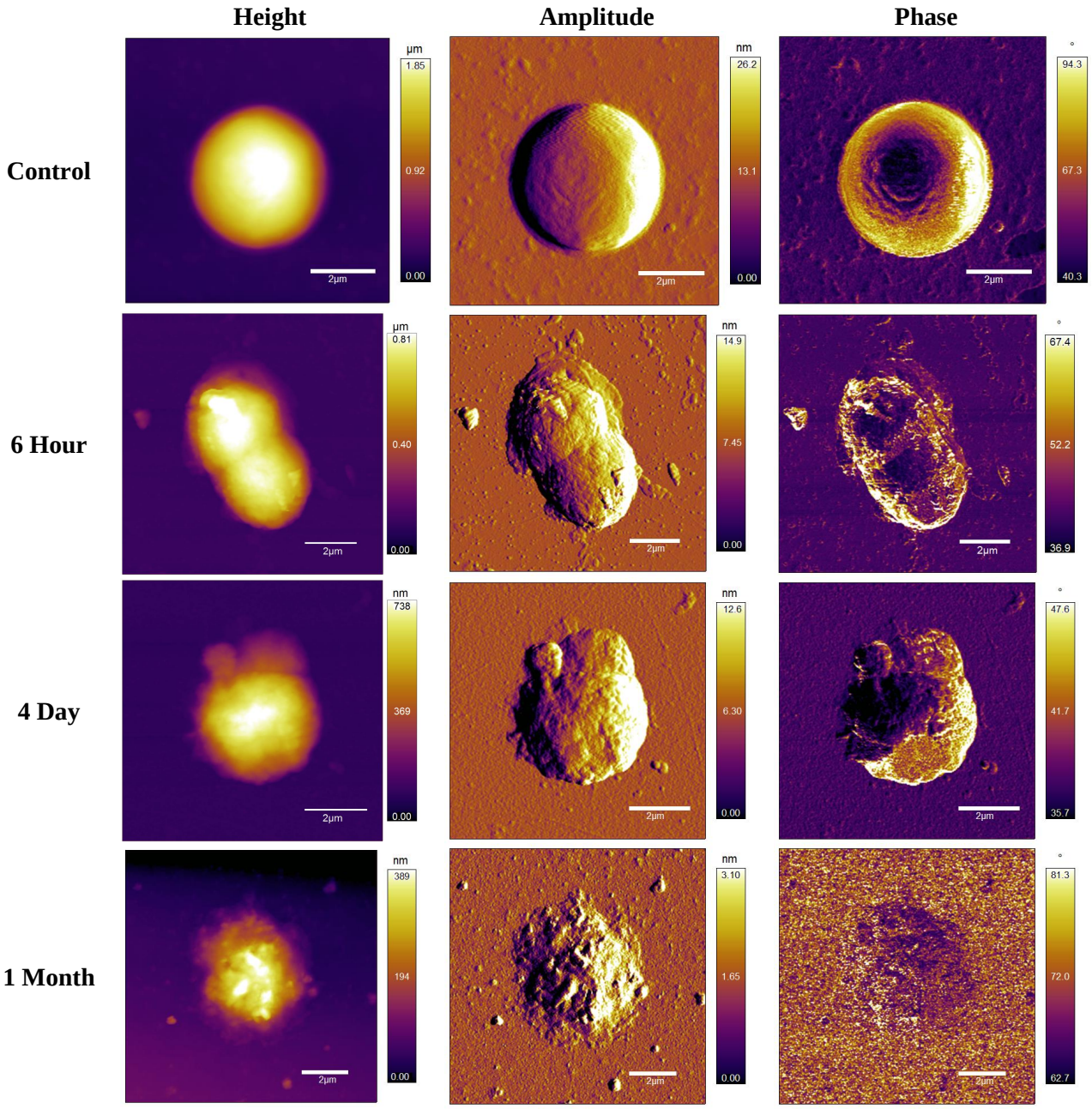

Figure 18: AC Air Tapping Mode (Height, Amplitude, Phase) of the lytic *Microcystis aeruginosa* - Ma-LEP relationship.

The morphological change of *Microcystis aeruginosa* after infection of Ma-LEP over 1 month shows structural damage. In the first column of Fig. 17, a definitive height decrease of about 1.5 µm can be seen over the span of 1 month. The initial height of *Microcystis aeruginosa* was measured to be 1.850 µm tall from the sample surface. The height decreased to .810, .738, and .389 after 6 hours, 4 days, and 1 month, respectively. The Amplitude values from the second column also decrease from 26.2, 14.9, 12.6, and then 3.1 nm for the Control, 6 hour, 4 day, and 1 month samples, respectively, indicating lower topographical variation over time. Lastly, the phase images show an increasing repulsiveness in the sample, showing change in stiffness properties over time. There are initially high attractive forces (yellow) with phases over 90 in the control sample, but after 1 month, these attractive forces are dispersed throughout the sample and are dominated by the repulsive region (purple).

Table 3: Results of AC Air Tapping Mode among the four time samples.

Sample	Height (µm)	Max Amplitude (nm)	Phase (degrees)
Microcystis aeruginosa (control)	1.850	26.2	40.3 – 94.3
6 hour incubation of *Microcystis aeruginosa* with Ma-LEP	0.810	14.9	36.9 – 67.4
4 day incubation of *Microcystis aeruginosa* with Ma-LEP	0.738	12.6	35.7 – 47.6
1 month incubation of *Microcystis aeruginosa* with Ma-LEP	0.389	3.1	62.7 – 81.3

In addition, potential phage patterns were also examined using AC Air Tapping Mode. Samples 2 week lysed *Microcystis* and Ma-LEP were scanned for evidence of cyanophage attacking the

cyanobacteria. The following pattern was found on the sample in several scanning locations. The following phage specimen images correspond to the locations specified in the 10x10 µm Amplitude image:

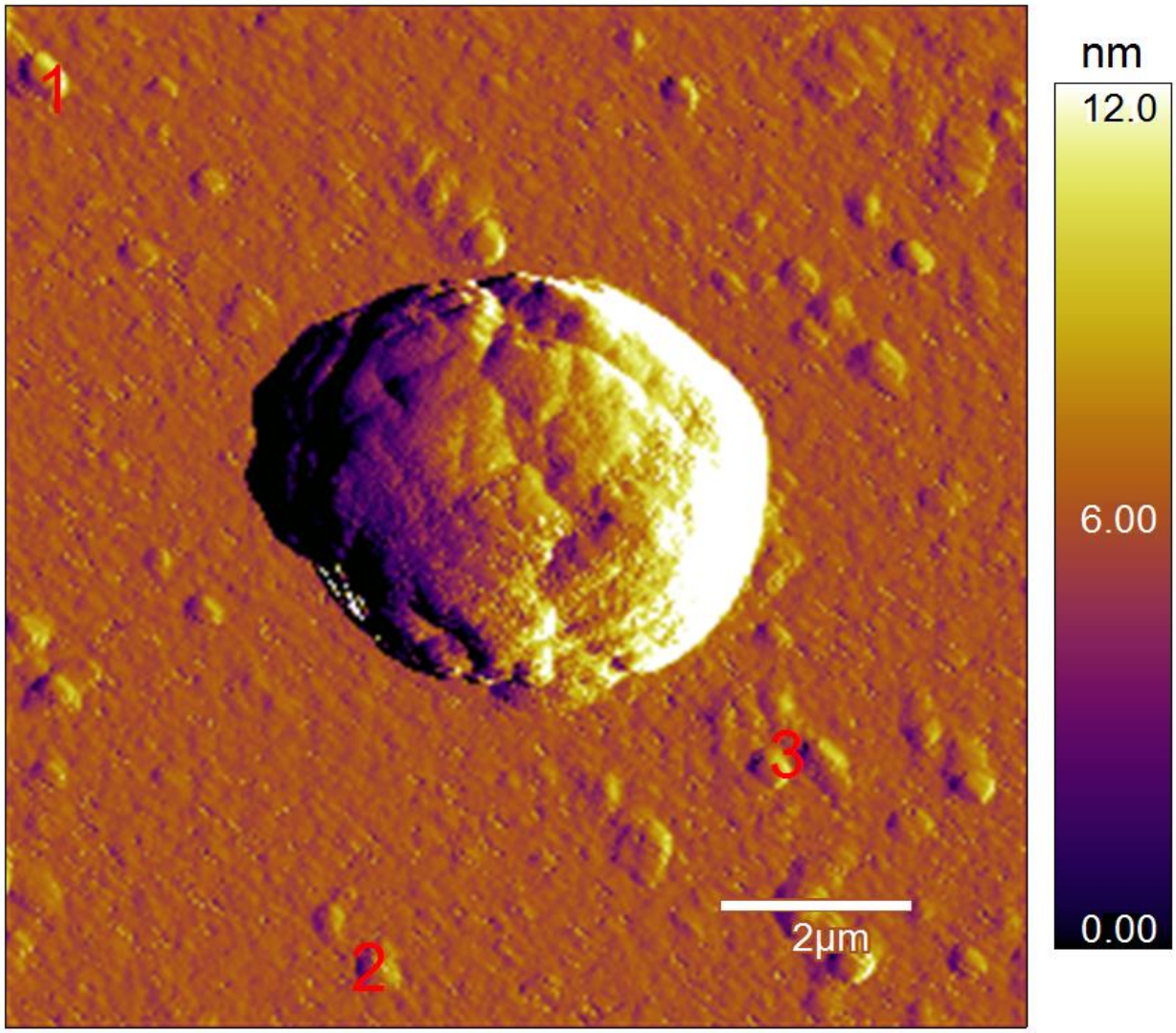

Figure 19: Specified phage specimens scanned with AC Air Tapping Mode (10x10 µm).

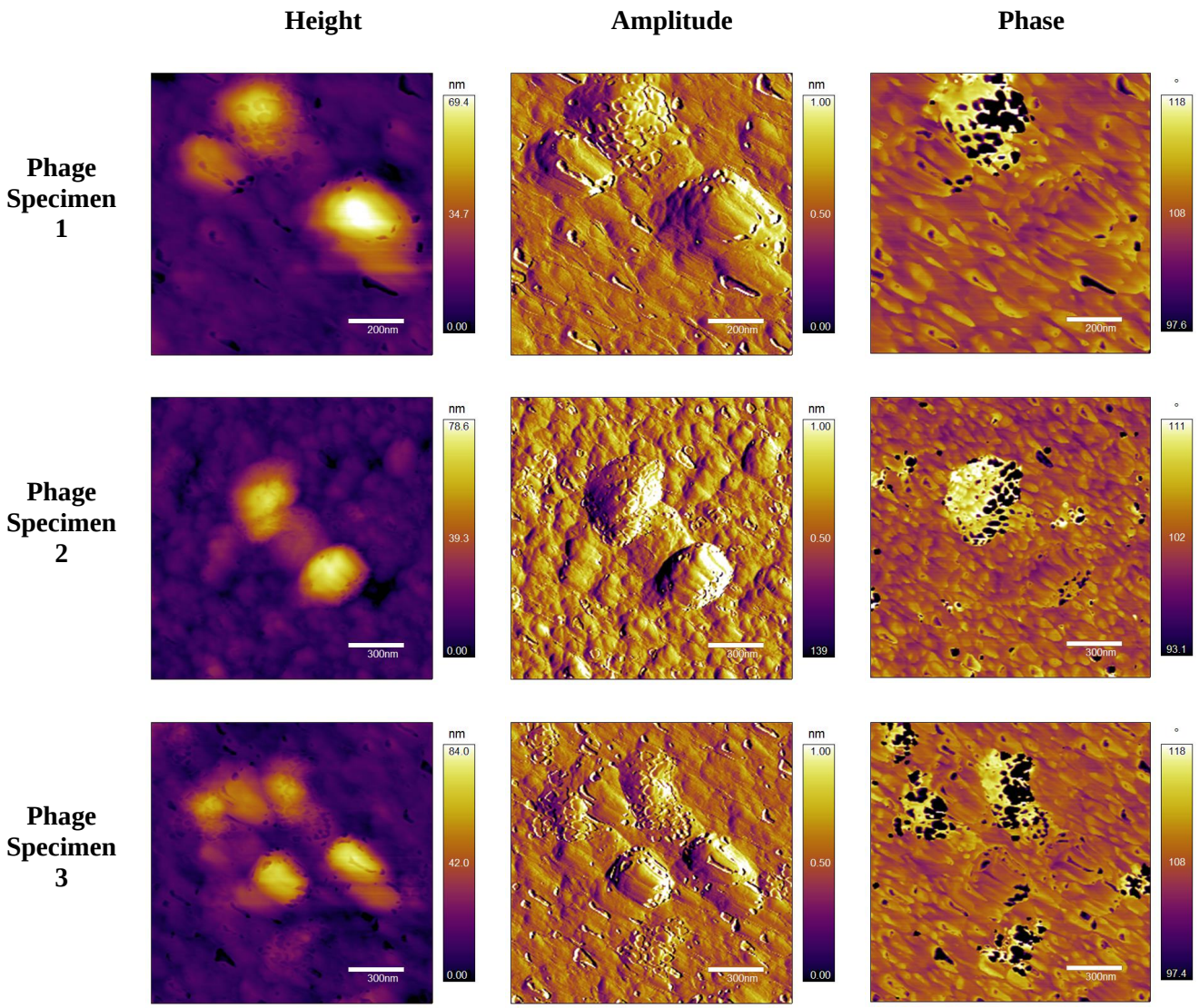

Figure 20: Height, Amplitude, and Phase images of Phage Specimens specified in Fig.19.

The Phage Specimens in Fig. 19 show similar characteristics. Each have similar heights, amplitudes, and phases. In addition, these images also show the potential phage specimens have a "head and tail" structure, which could potentially give information on the attacking end of the phage. Evidence of this phage during lysis of *Microcystis* is also investigated in AFM-IR Spectroscopy section of the results.

4.2 AM-FM Viscoelastic Tapping Mode

Scans of 5-10 areas were performed on each time sample to find a representative sample for the population. Figure 18 shows the representative samples at each sample time.

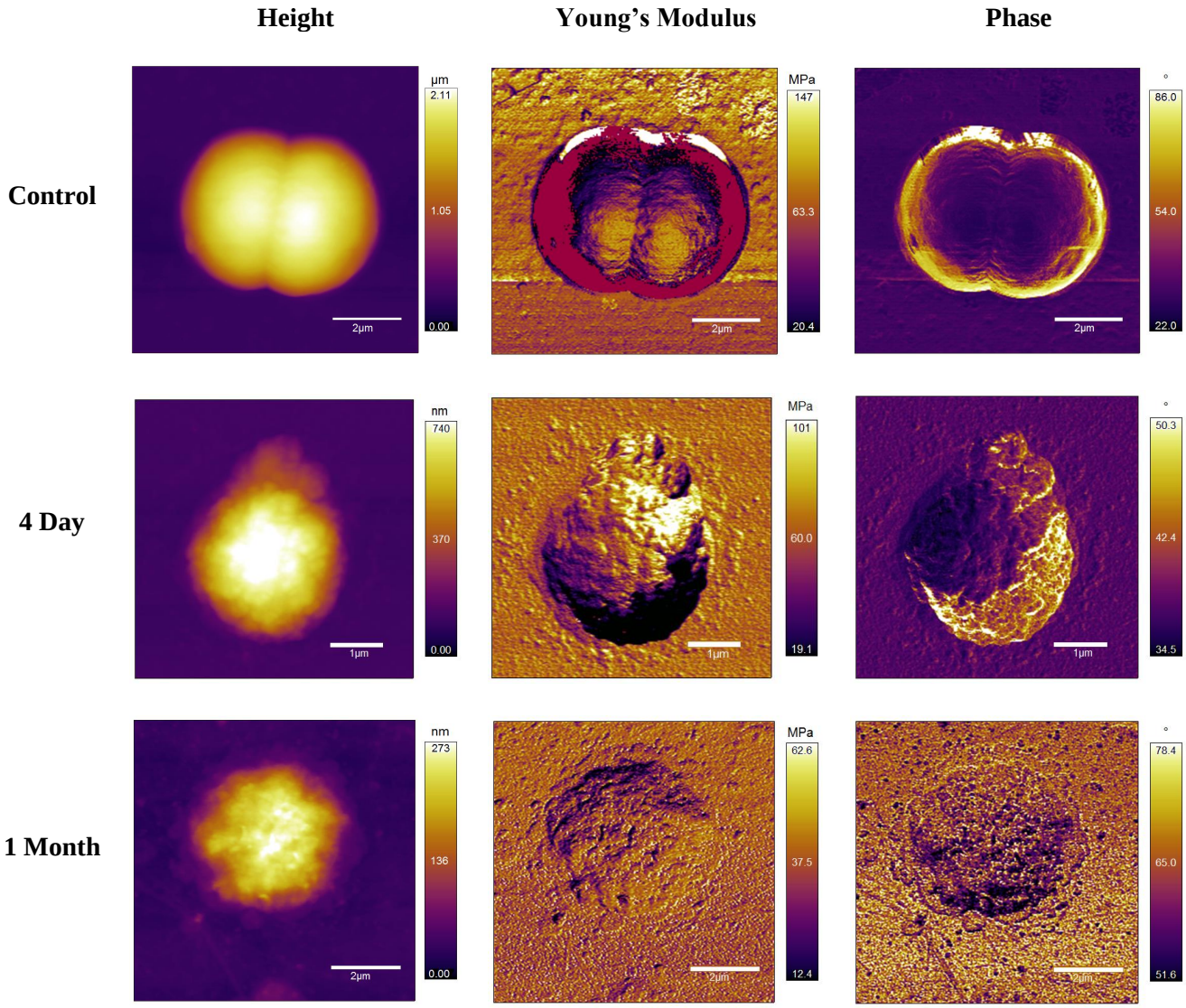

Figure 21: AM-FM Viscoelastic Mapping Mode (Height, Young's Modulus, Phase) of the lytic *Microcystis aeruginosa* – Ma-LEP relationship.

The results from the AM-FM Viscoelastic Tapping Mode show similar results in terms of height and phase as the previous AC Air Tapping Mode. Height images over 1 month showed the same trend and similar sizes, decreasing from 2.110 µm to 0.273 µm over 1 month. The

phase showed similar range decrease, showing large areas of attraction initially but eventually becoming dominantly repulsive after 1 month. The Young's Modulus measurements of AM-FM show the same trend. The maximum Young's Modulus value in the control sample starts at 147 MPa, decreasing to 101 MPa after 4 days and 62.6 MPa after 1 month. In addition, it is important to point out the 4 day sample in this experiment, as it shows significant material changes between the upper and lower halves of the sample. This is proved again through the AM-FM measurement of Young's modulus, showing the upper half has relatively higher Young's Modulus values between 60.0 – 101 MPa, while the lower half has very low Young's Modulus values at 19.1 MPa. Lastly, the phage images show a similar trend to those in the AC Air Tapping Mode Results. The control phase ranges from 22.0 to 86.0 degrees, shrinks to a range of 34.5 to 50.3 degrees, then raises to a range of 51.6 to 78.4 due to the dissipation of the cyanobacteria.

Table 4: Results of AM-FM Viscoelastic Mapping Mode among the three time samples.

Sample	Height (μm)	Max Young's Modulus (MPa)	Phase (degrees)
Microcystis aeruginosa (control)	2.110	147	22.0 – 86.0
4 day incubation of *Microcystis aeruginosa* with Ma-LEP	0.740	101	34.5 – 50.3
1 month incubation of *Microcystis aeruginosa* with Ma-LEP	0.273	62.6	51.6 – 78.4

4.3 AFM-IR Spectroscopy

Samples were sent in September and are currently queued. Results are expected sometime in November. We expect to see a chemical composition difference between the cyanobacteria before and after lysis. Additionally, we expect to see chemical evidence of the phage on the lysed cyanobacteria sample. Using the resonance frequencies found from the isolated phage sample, these resonance frequencies can be searched for on the lysed cyanobacteria sample.

4.4 Liquid AFM

Preliminary Liquid AFM scans of *Microcystis* unexposed to Ma-LEP showed higher resolution due to the lower scanning rate required for in-liquid measurement. A representative cyanobacteria can be seen in Fig. 21:

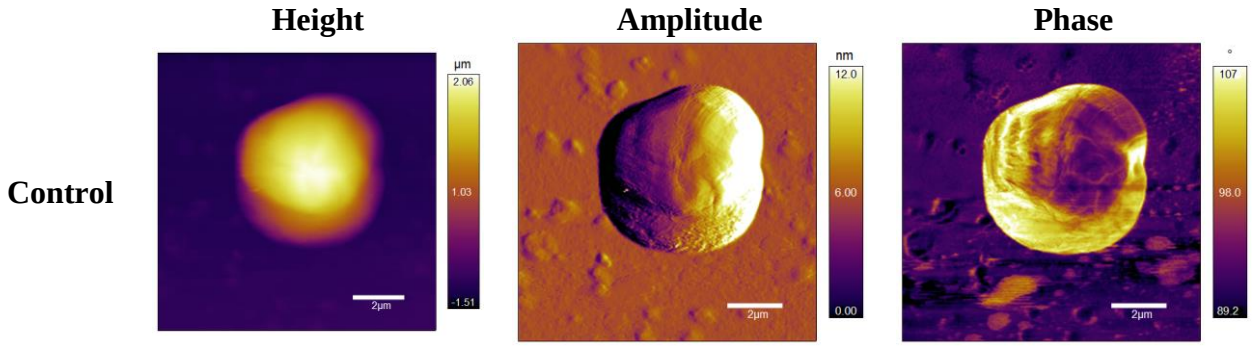

Figure 22: Preliminary Liquid AFM scans of Microcystis aeruginosa control sample (10x10).

Current *in-situ* scans of the lytic *Microcystis aeruginosa* and Ma-LEP relationship are being performed. Initial measurements showed little to no lytic evidence when the control sample is exposed to phage at a ratio of 10:1 medium to phage solution. This ratio has been increased to 10:2 or 10:3 medium to phage solution in order to show lysis of the cyanobacteria.

Chapter 5: Conclusion

Cyanophage Ma-LEP showed lytic behavior when infecting to *Microcystis aeruginosa.* The lytic cycle between the two organisms characterized through time, height, phase, and Young's modulus, showing overall degradation of the cyanobacterial structure. By better understanding the lytic cyanobacteria – cyanphage relationship, the cyanophage can be used in larger populations of *Microcystis aeruginosa* to see its effects on mass populations.

Chapter 6: Future Work

6.1 Creation of "Mini-Biome"

The role of Liquid AFM is to simulate the ecosystem of the cyanobacteria *Microcystis aeruginosa* and cyanophage Ma-LEP. One of the goals of this experiment during its conception was to add several attachments during Liquid AFM scanning such as heated stage and UV light. Adding these factors allows simulating lake temperature and UV exposure of HABs. A rate of degradation has been found without these factors – adding them *in-situ* would give a more accurate rate of degradation.

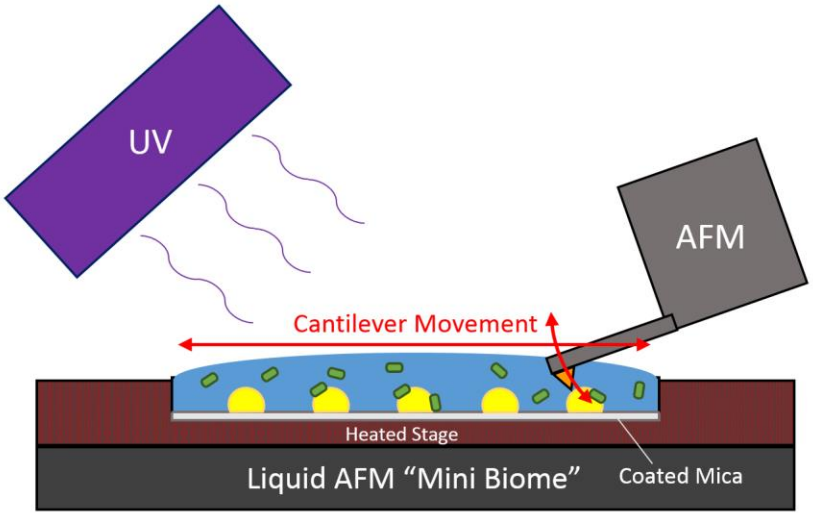

Figure 23: Liquid "Mini-Biome" Schematic

6.2 Video-Rate AFM

In late October, Asylum Research came to Ohio State to demo the new Cypher VRS, a Video-Rate AFM. For liquid images in this experiment, scans were taken at .2 Hz (scanning duration of about 1.5 hours). The Video-Rate AFM has capabilities of scanning from 20 to 40 Hz, 100-200 times the speed of our current Liquid AFM measurements. One limitation of this

method is the height of samples – current height limitations, according to Asylum Research, of the Cypher VRS is about 2.5 µm. The height of *Microcystis aeruginosa* (control) in this experiment was found to be around 2-2.5 µm, which would pose a problem during rapid scanning. If this method of AFM develops to scan taller samples in the near future, then it would be the perfect tool to view lytic behavior of the *Microcystis aeruginosa* – Ma-LEP relationship [27].

6.3 Biocontrol Development

On a larger scale, the purpose of characterizing lytic behavior of Ma-LEP is to develop the cyanophage into a biocontrol. After fully understanding its behavior while interacting with *Microcystis aeruginosa*, it should be tested in larger populations to simulate how it would perform in Lake Erie. Variables such as the amount of phage needed to degrade a measured amount of cyanophage must be researched to apply it in actual environments in the future.

References

[1] S. D. S. M. S. Masten, Flint Water Crisis: What Happened and Why?, vol. 108(12), J Am Water Works Assoc., 2016, pp. 22-34.

[2] U. S. E. P. Agency, "Great Lakes Facts and Figures," 2017. [Online]. Available: https://www.epa.gov/greatlakes/great-lakes-facts-and-figures.

[3] N. E. Observatory, "Image of the Day," 5 October 2011. [Online]. Available: https://earthobservatory.nasa.gov/IOTD/view.php?id=76127.

[4] O. D. o. Health, "Harmful Algal Blloms," 2017. [Online]. Available: https://www.odh.ohio.gov/odhprograms/eh/HABs/algalblooms.aspx.

[5] U. S. E. P. Agency, "Harmful Algal Blooms," 2017. [Online]. Available: https://www.epa.gov/nutrientpollution/harmful-algal-blooms#learn.

[6] E. Wilson, "Danger from microcystins in Toledo water unclear," *Chem. Eng. News*, vol. 92, no. 32, p. 9.

[7] W. Carmichael, "Toxic Microcystis and the Environment," in *Toxic Microcystis*, Boca Raton, CRC Press, 1995, pp. 1-12.

[8] M. Hallegraeff, "A review of harmful algal blooms and their apparent global increase.," *Phycologia,* vol. 32, no. 2, pp. 79-99, 1993.

[9] P. Hoagland, D. Anderson, Y. Kaoru and A. White, "The Economic Effects of Harmful Algal Blooms in teh United States: Estimates, Assessment Issues, and Information Needs," *Estuaries,* vol. 25, no. 4b, pp. 819-837, 2002.

[10] B. Whitton and M. Potts, "Chapter 1: Introduction to the Cyanobacteria," in *The Ecology of Cyanobacteria: Their Diversity in Time and Space*, Springer, 2000, pp. 1-9.

[11] L. Blaha, P. Babica and B. Marsalek, "Toxins produced in cyanobacterial water blooms - toxicity and risks," *Interdiscip. Toxicol.,* vol. 2, no. 2, pp. 36-41, 2009.

[12] A. Humpage, M. Fenech, T. P and F. IR, "Micronucleus induction and chromosome loss in transformed human white cells indicate clastogenic and aneugenic action of the cyanobacterial toxin, cylindrospermopsin.," *Mutation Research/Genetic Toxicology and Environmental Mutagenesis.,* vol. 472, pp. 155-161, 2000.

[13] T. Duy, P. Lam, G. Shaw and C. D.W., "Toxicology adn risk assessment of freshwater cyanobacterial (blue-green algal) toxins in water.," *Rev Environ Contam Toxicol,* vol. 163, no. 113, p. 85, 2000.

[14] B. Cummings, "Lytic and Lysogenic Cycles," Pearson Eductation, Inc., 2004. [Online]. Available: http://lh6.ggpht.com/-ezqWWBNtWQc/UThK7PGNYQI/AAAAAAAAE3Y/RZNa1X7x26w/lytic%252520and%252520lysogenic%252520cycle_thumb%25255B5%25255D.jpg?imgmax=800.

[15] N. Mann and M. Clokie, "Chapter 21: Cyanophages," in *The Ecology of Cyanobacteria*, Springer, 2002, pp. 367-395.

[16] ThermoFisher Scienteific, "An Introduction to Electron Microscopy," ThermoFisher Scientific, 2017. [Online]. Available: https://www.fei.com/introduction-to-electron-microscopy/sem/.

[17] Olympus, "OMCL-AC240TS," Olympus, 2017. [Online]. Available: http://probe.olympus-global.com/en/product/omcl_ac240ts_r3/.

[18] A. Research, "Applications," Oxford Instruments, 2017. [Online]. Available: https://www.asylumresearch.com/Applications/Applications.shtml#G.

[19] A. Reseearch, "AC Imaging (Tapping Mode) Tutorial," Oxford Instruments, 2017. [Online]. Available: https://www.oxford-instruments.com/businesses/nanotechnology/asylum-research/afm-video-tutorials/oi/tapping-mode-tutorial.

[20] "Phase Imaging/Chemical Mapping," Advanced Surface Microscopy, Inc., 2015. [Online]. Available: http://www.asmicro.com/applications/phase.htm.

[21] D. Hurley, M. Kocun, I. Revenko, B. Ohler and R. Proksch, "Fast, quantitative AFM nano-mechanical measurements using AM-FM Viscoelastic Mapping Mode," *Microscopy and Analysis,* vol. March/April 15, pp. 9-13, 2015.

[22] "AFM-IR: Breakthrough nanoscale infrared spectroscopy for organics, polymers and life sciences," ANASYS Instruments, 2017. [Online]. Available: https://www.anasysinstruments.com/afm-ir-overview/.

[23] "Commercial AFMs," Nanoscale Function Group, 2013. [Online]. Available: http://www.nanofunction.org/p/commercialafms.

[24] J. X, L. S, J. Kwon, G. T, H. Cho and J. Lee, "Isolation and characterization of cyanophages infecting Microcystis aeruginosa in Lake Erie for potential biological control of HABs," in *Understanding Algal Blooms: State of the Science Conference,* Toledo, OH, 2016.

[25] E. Haramoto, H. Katayama, K. Oguma and S. Ohgaki, "Application of Cation-Coated Filter Method to Detection of Noroviruses, Enteroviruses, Adenoviruses, and Torque

Teno Viruses in the Tamagawa River in Japan," *Applied and Environmental Microbiology,* vol. 71, no. 5, pp. 2403-2411, 2005.

[26] D. Allison, C. Sullivan, N. Mortensen, S. Retterer and M. Doktycz, "Bacterial immobilization for imaging by atomic force microscopy," *J Vis Exp,* vol. 54, p. 2880, 2011.

[27] A. Research, "Video-Rate AFM Workshop," in *Lectuer and Equipment Demonstration in Scott Laboratory*, Columbus, OH, 2017.

Appendix A: Expanded Images

Figure 24

18.1 Height Images

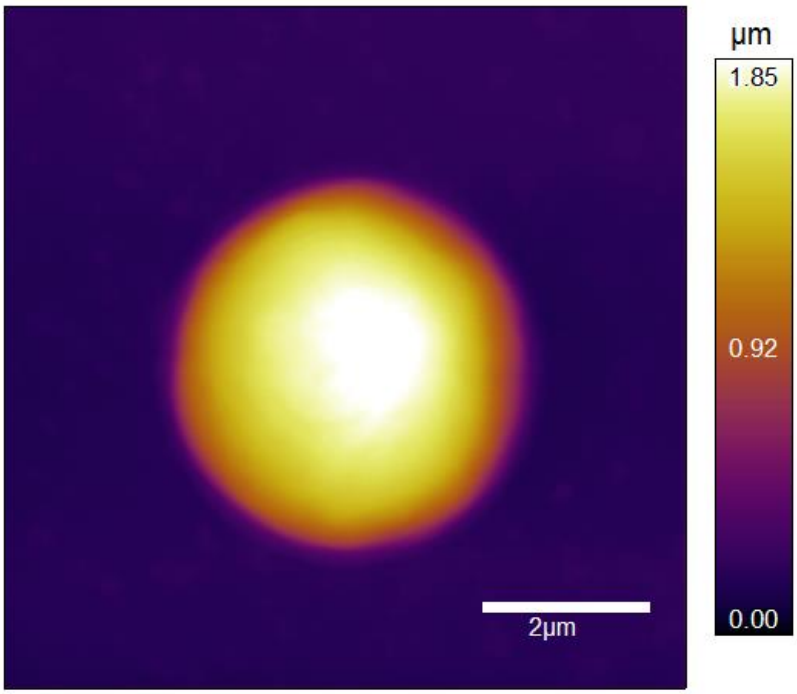

Figure A 1: *Microcystis aeruginosa* (control), 10x10 µm.

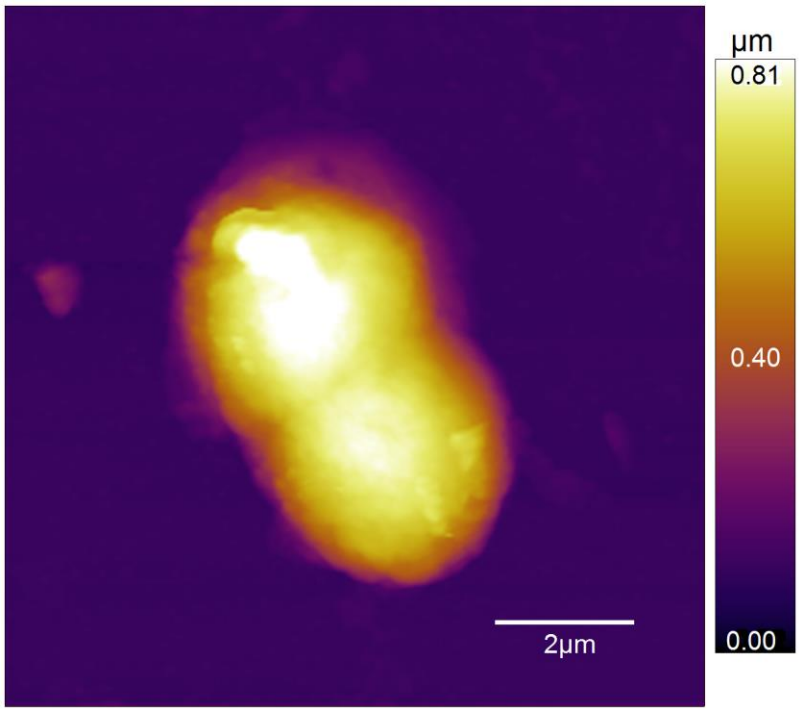

Figure A 2: 6 hour incubation of *Microcystis aeruginosa* with Ma-LEP, 10x10 µm.

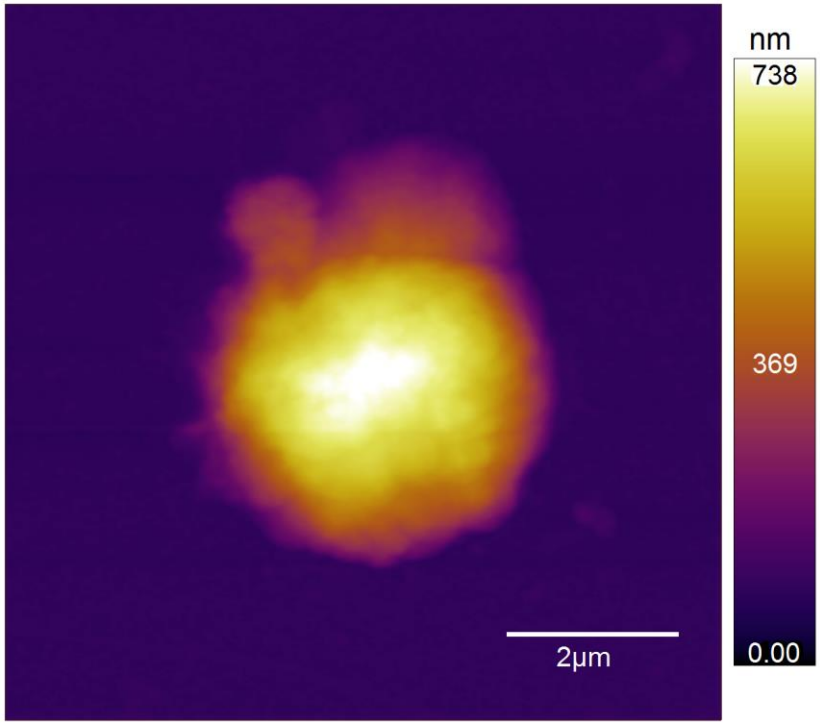

Figure A 3: 4 day incubation of *Microcystis aeruginosa* with Ma-LEP, 10x10 µm.

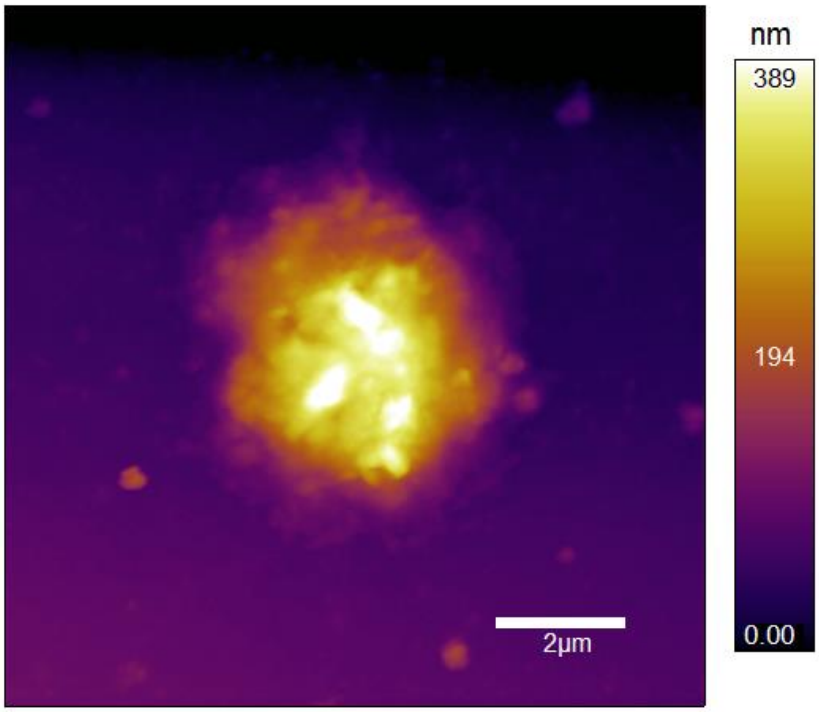

Figure A 4: 1 month incubation of *Microcystis aeruginosa* with Ma-LEP, 10x10 µm.

18.2 Amplitude Images

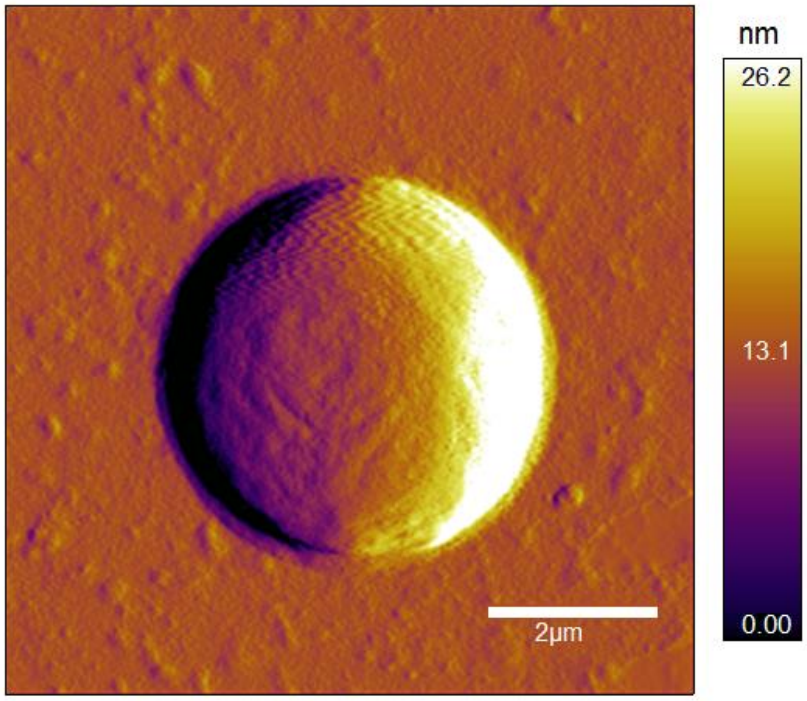

Figure A 5: *Microcystis aeruginosa* (control), 10x10 µm.

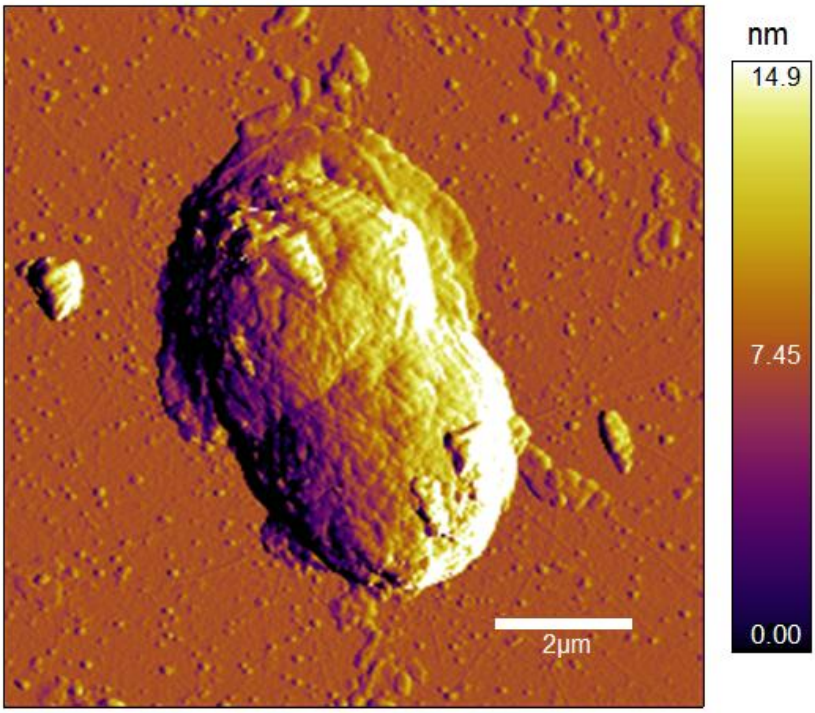

Figure A 6: 6 hour incubation of *Microcystis aeruginosa* with Ma-LEP, 10x10 µm.

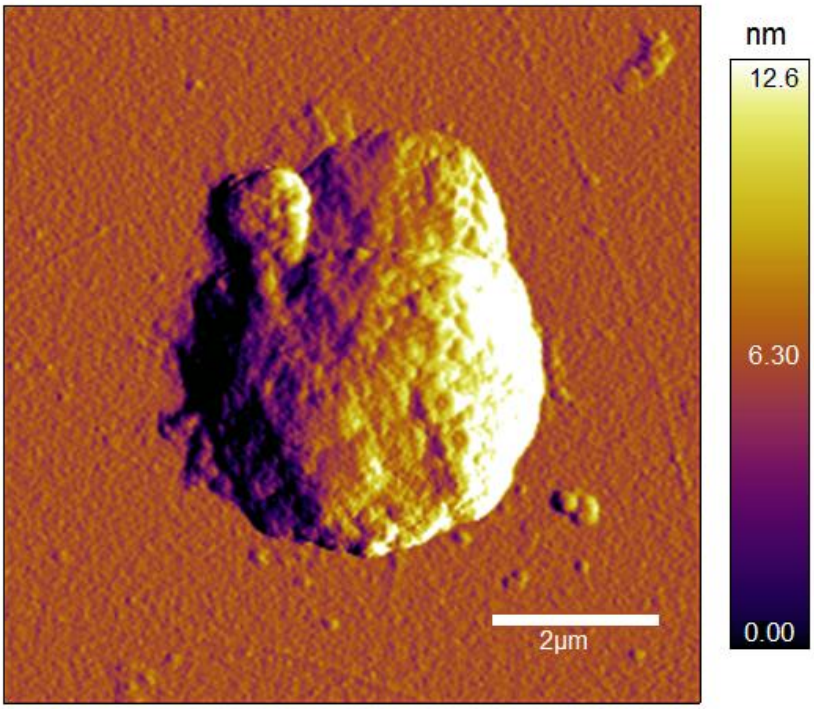

Figure A 7: 4 day incubation of *Microcystis aeruginosa* with Ma-LEP, 10x10 µm.

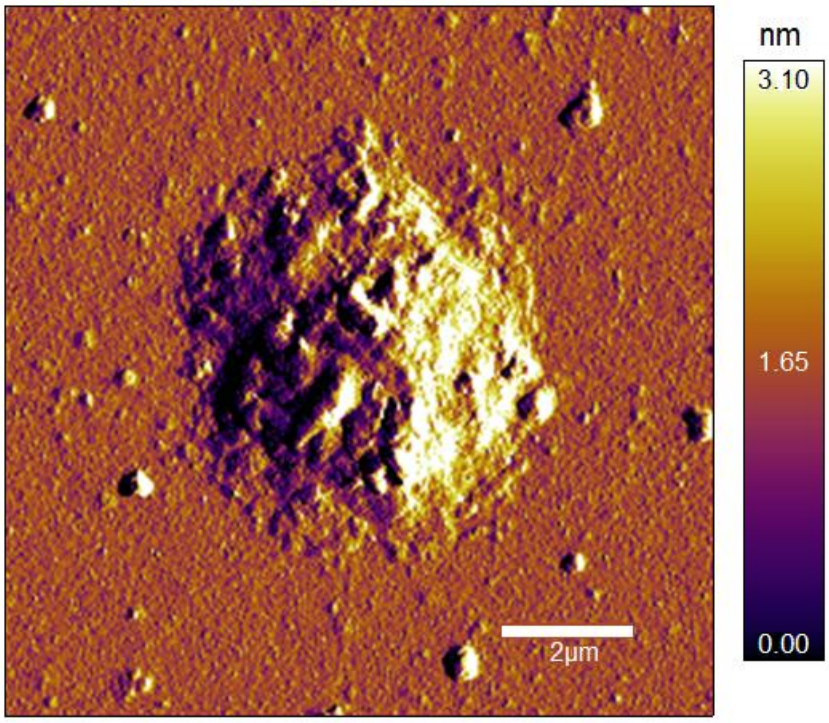

Figure A 8: 1 Month incubation of *Microcystis aeruginosa* with Ma-LEP, 10x10 µm.

18.3 Phase Images

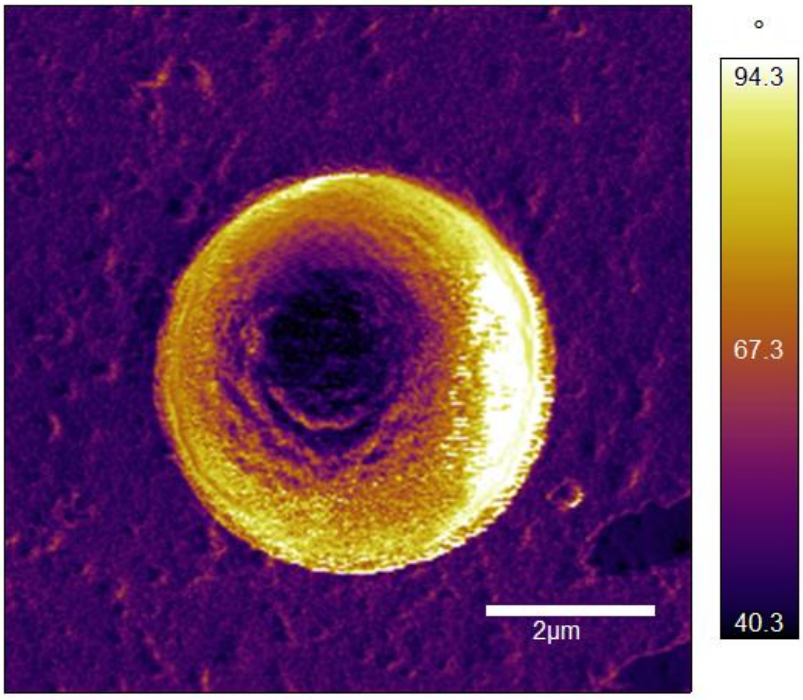

Figure A 9: *Microcystis aeruginosa* (control), 10x10 µm.

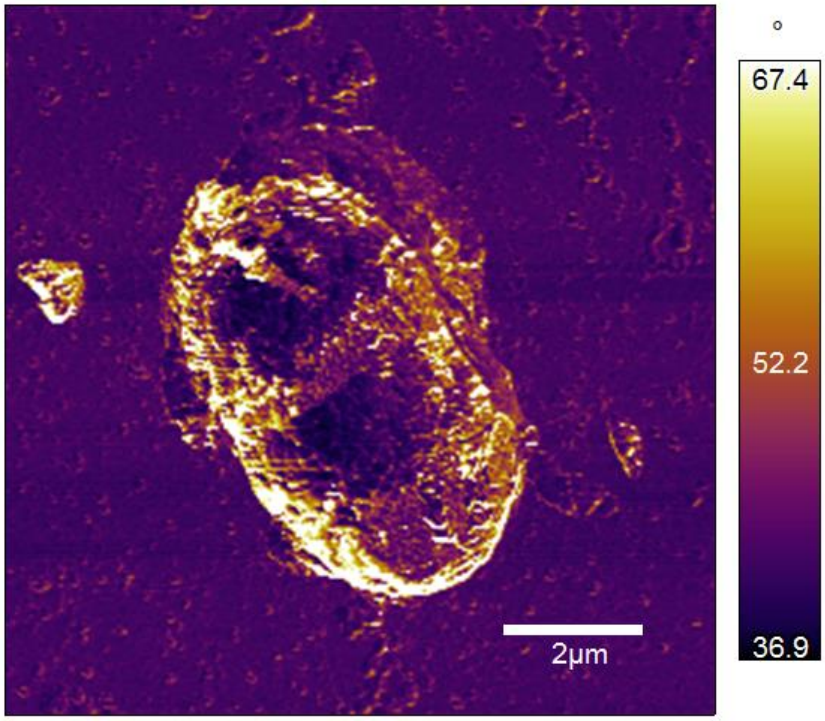

Figure A 10: 6 hour incubation of *Microcystis aeruginosa* with Ma-LEP, 10x10 µm.

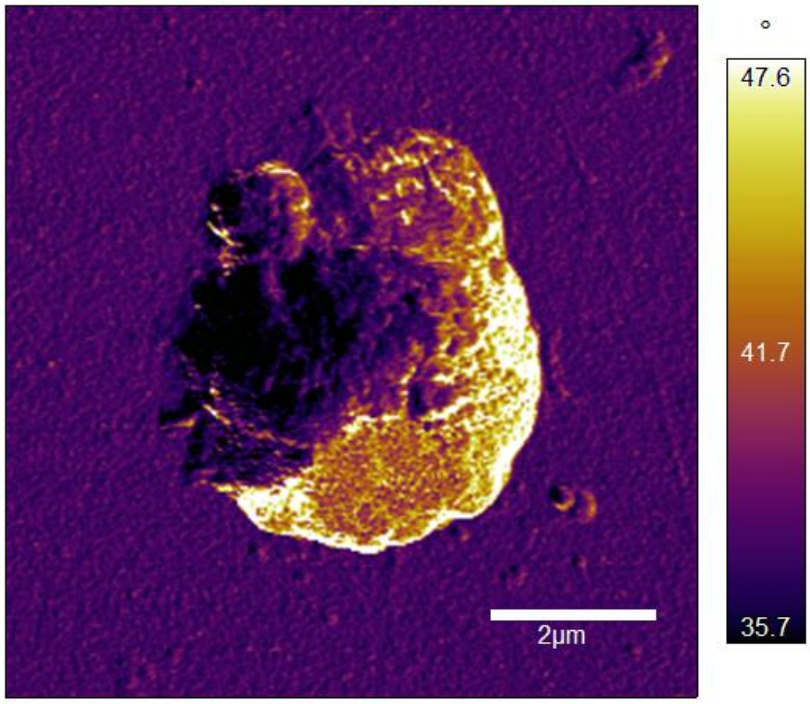

Figure A 11: 4 day incubation of *Microcystis aeruginosa* with Ma-LEP, 10x10 µm.

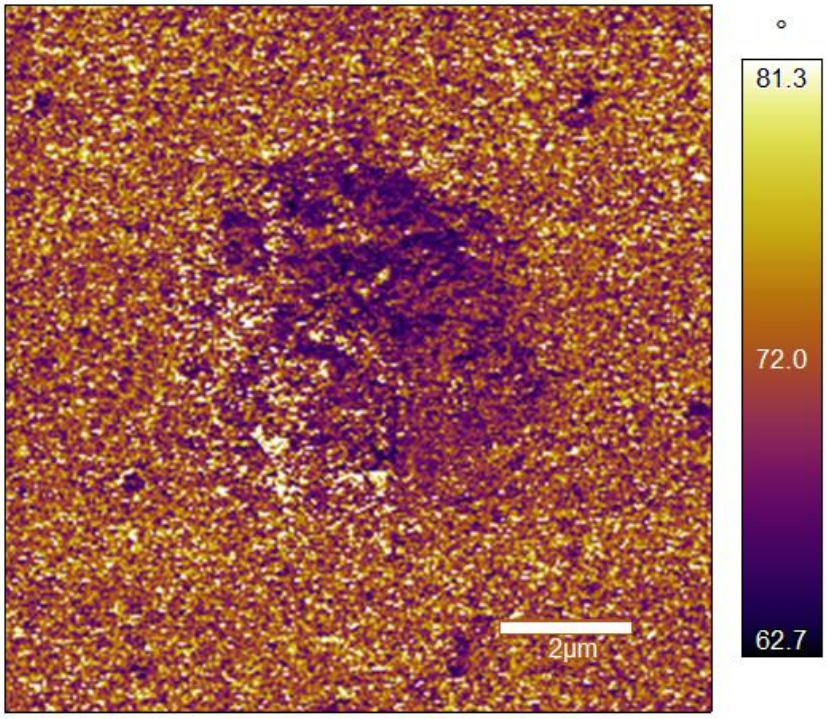

Figure A 12: 1 month incubation of *Microcystis aeruginosa* with Ma-LEP, 10x10 µm.

Figure 20

20.1 Height Images

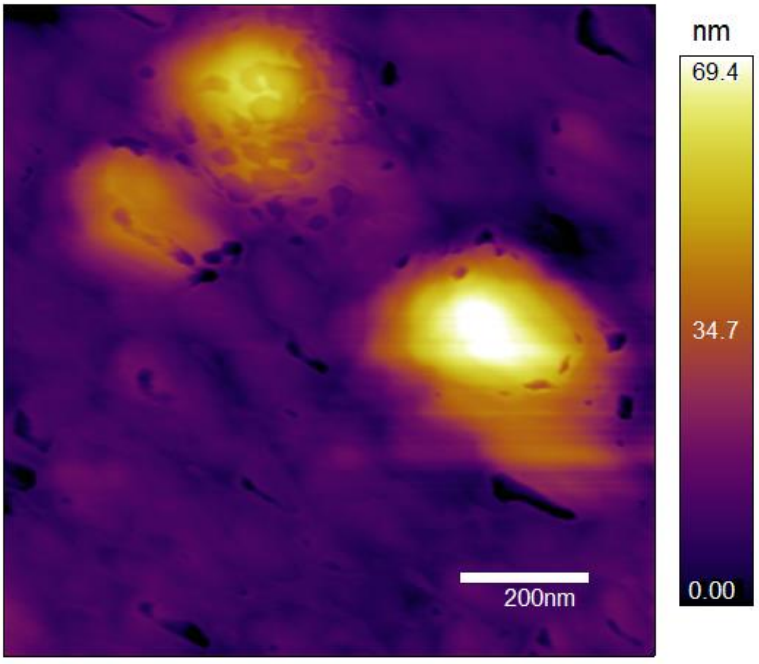

Figure A 13: Phage Specimen 1 (labeled) on Fig. 19, 1x1 µm.

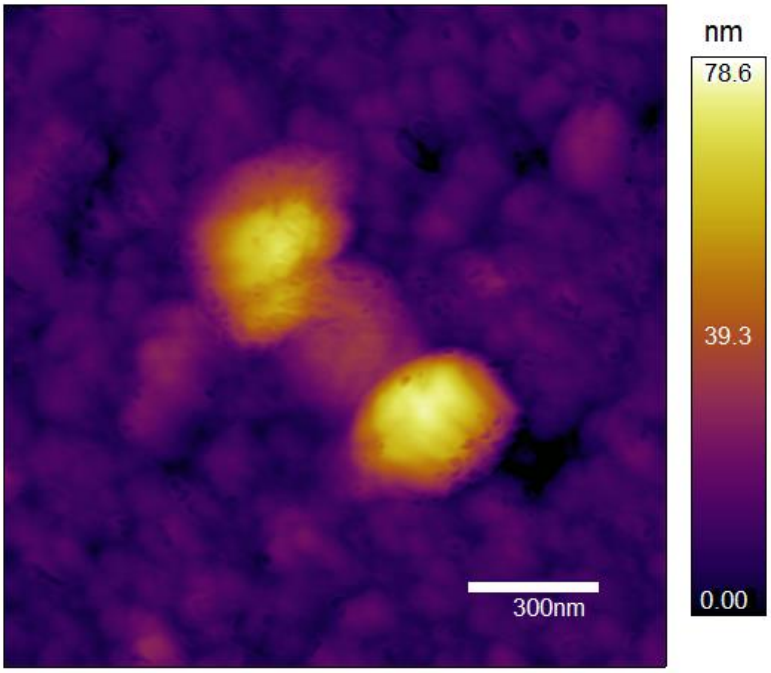

Figure A 14: Phage Specimen 2 (labeled on Fig. 19), 1.5x1.5 µm.

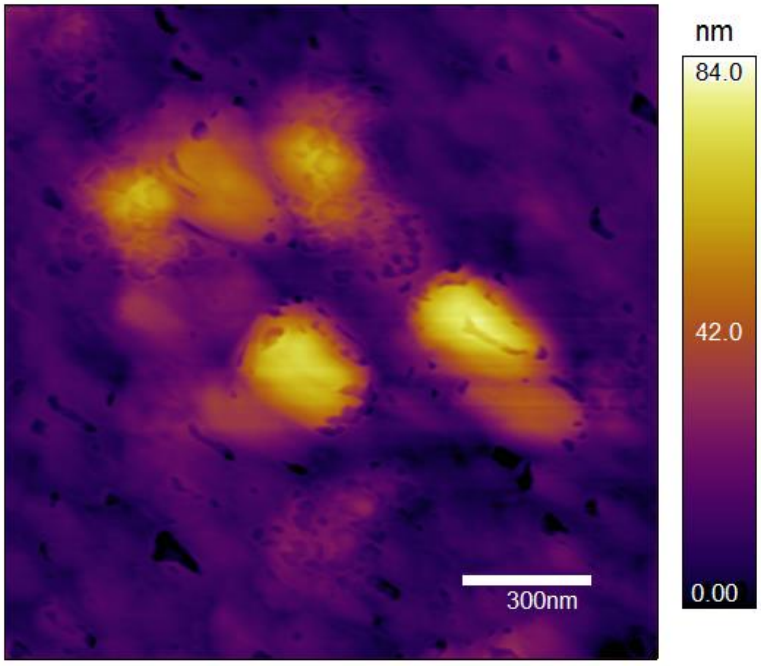

Figure A 15: Phage Specimen 3 (labeled on Fig. 19), 1.5x1.5 µm.

20.2 Amplitude Images

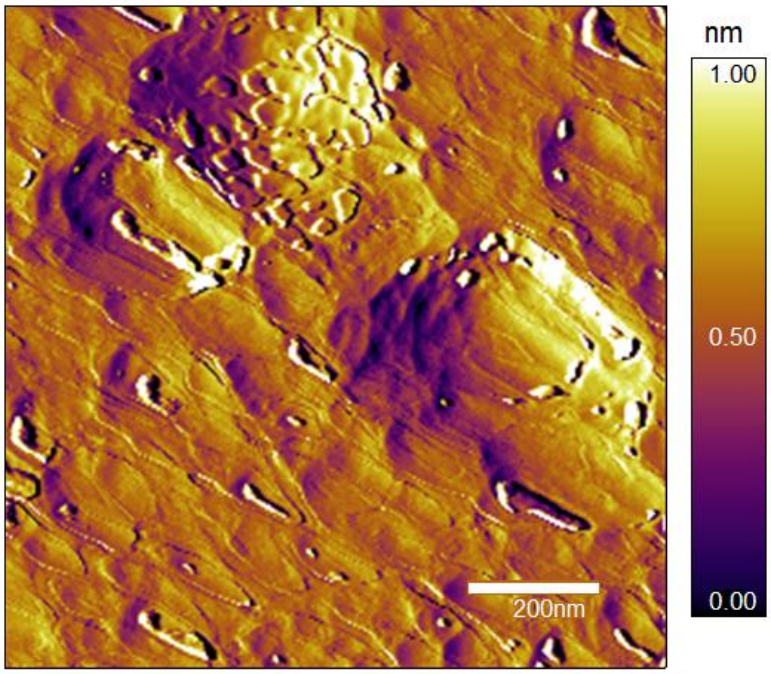

Figure A 16: Phage Specimen 1 (labeled on Fig. 19), 1x1 µm.

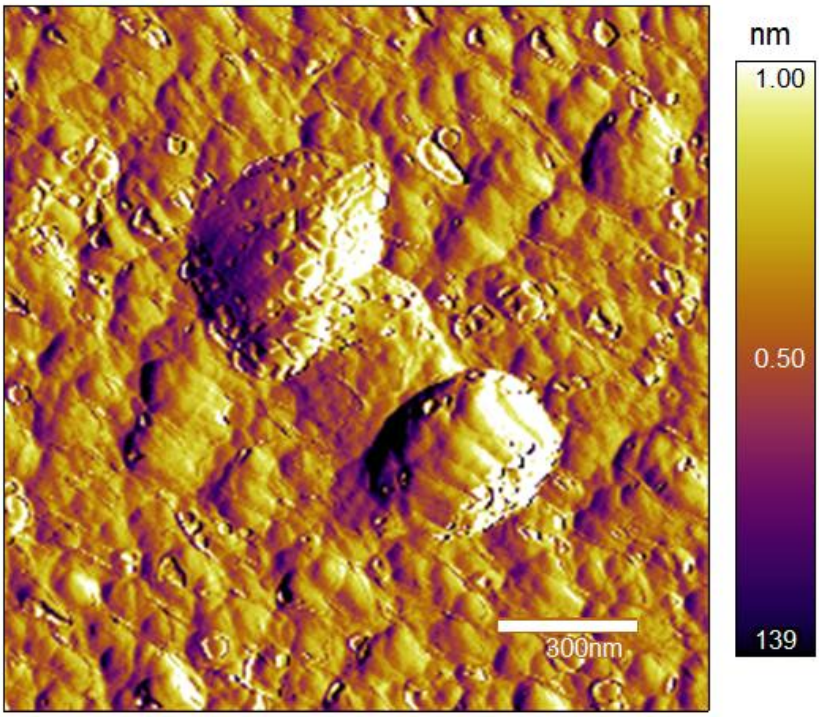

Figure A 17: Phage Specimen 2 (labeled on Fig. 19), 1.5x1.5 µm.

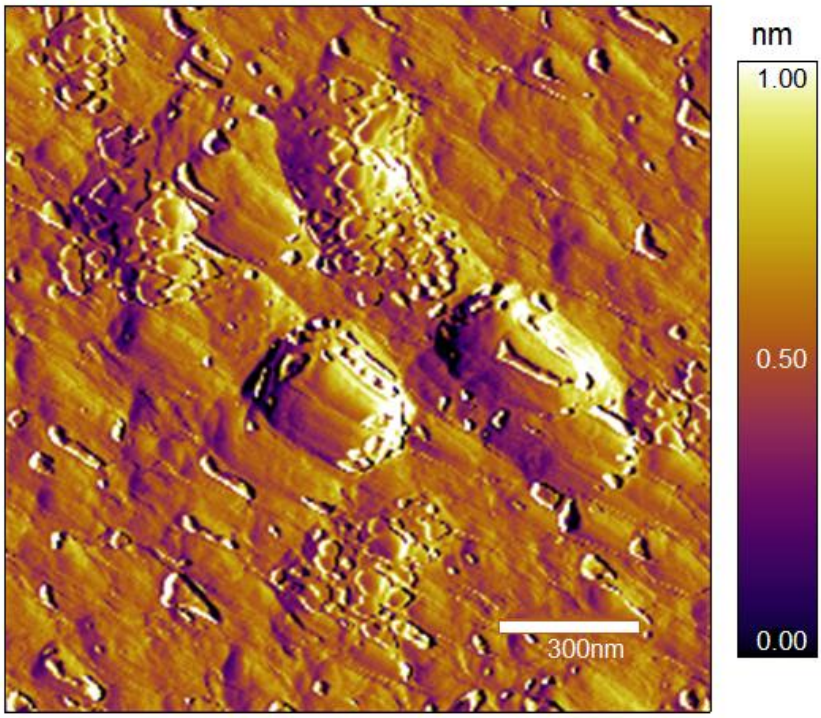

Figure A 18: Phage Specimen 3 (labeled on Fig. 19), 1.5x1.5 µm.

20.3 Phase Images

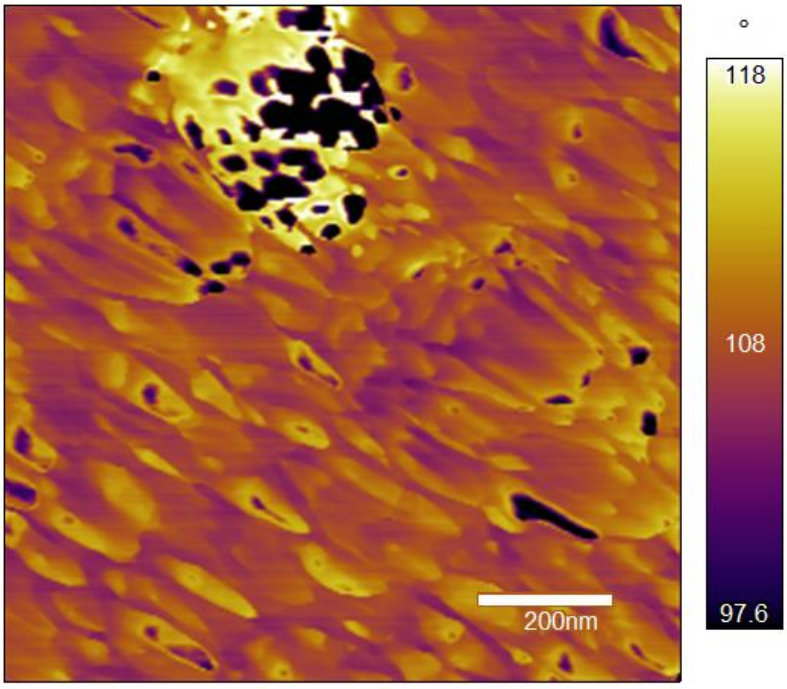

Figure A 19: Phage Specimen 1 (labeled on Fig. 19), 1x1 µm.

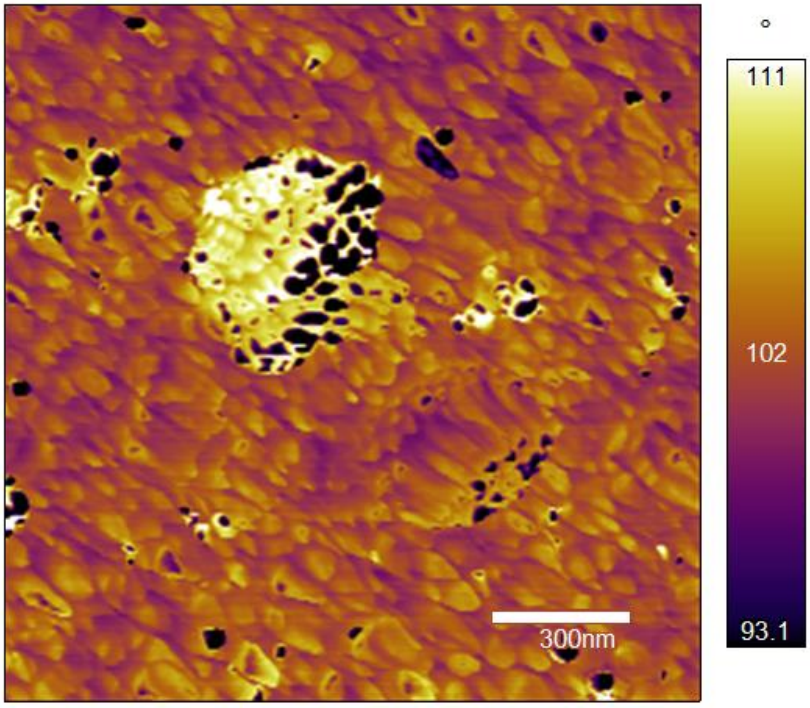

Figure A 20: Phage Specimen 2 (labeled on Fig. 19), 1.5x1.5 µm.

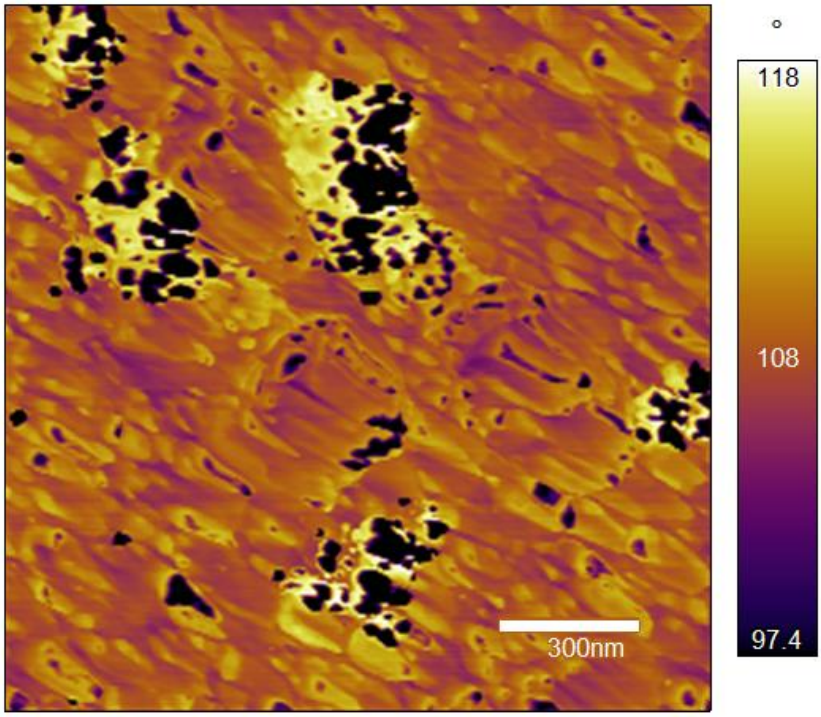

Figure A 21: Phage Specimen 3 (labeled on Fig. 19), 1.5x1.5 µm.

Figure 21

21.1 Height Images

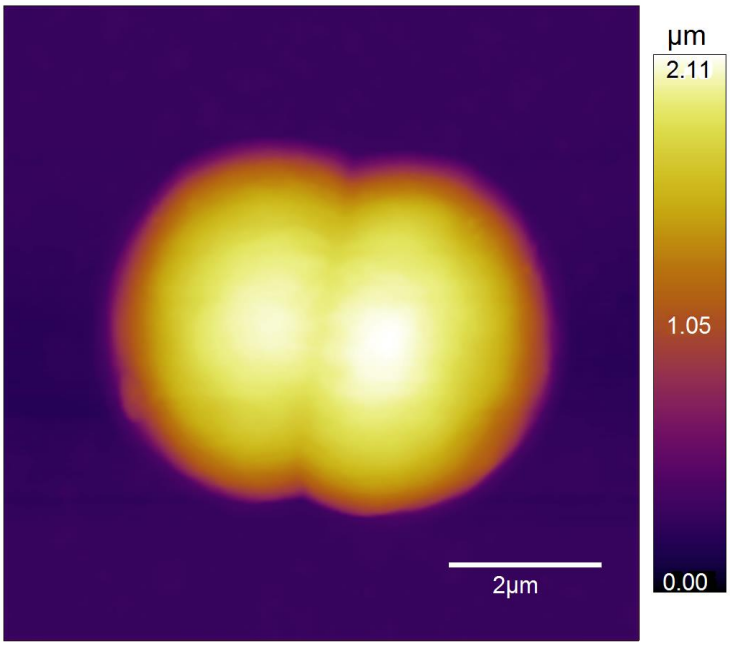

Figure A 22: *Microcystis aeruginosa* (control), 10x10 µm.

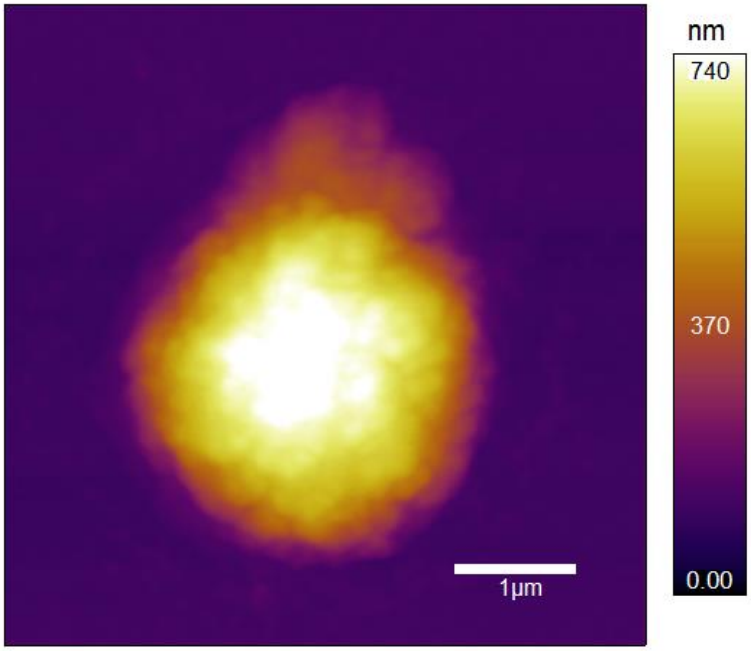

Figure A 23: 4 day incubation of *Microcystis aeruginosa* with Ma-LEP, 5x5 µm.

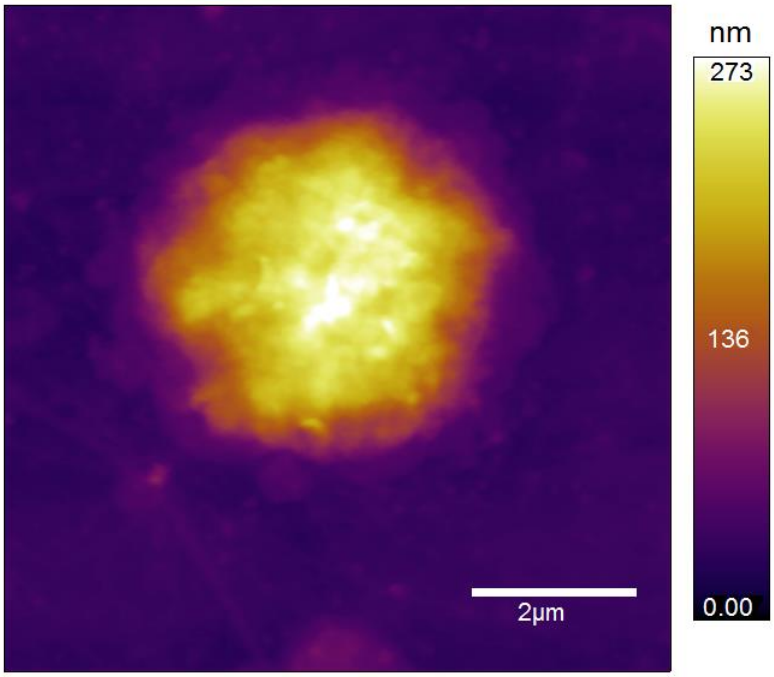

Figure A 24: 1 month incubation of *Microcystis aeruginosa* with Ma-LEP, 10x10 µm.

21.2 Young's Modulus Images

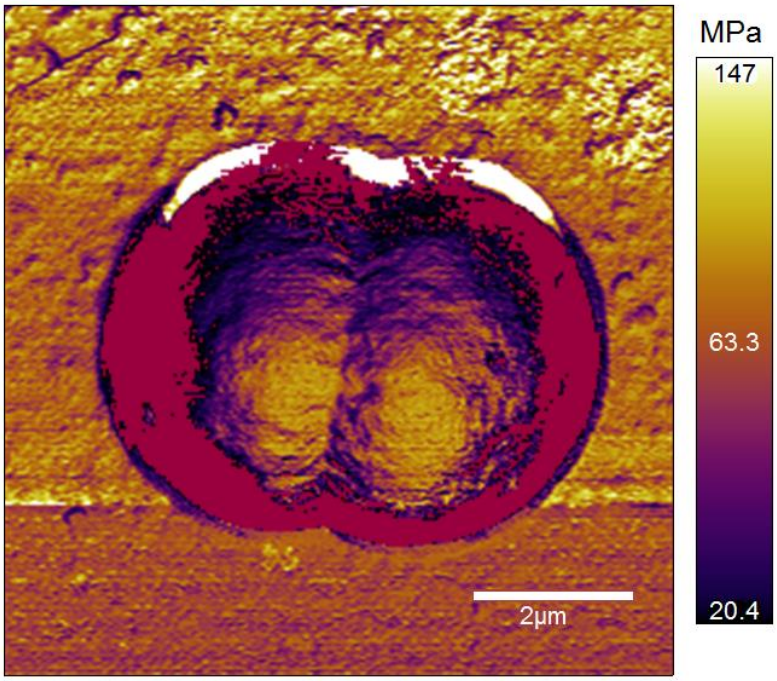

Figure A 25: *Microcystis aeruginosa* (control), 10x10 µm.

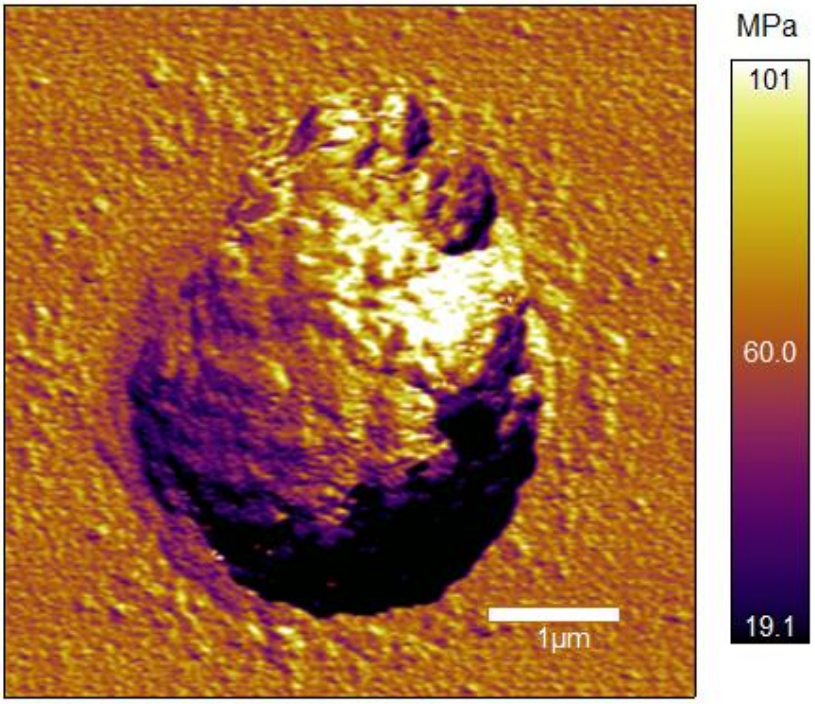

Figure A 26: 4 day incubation of *Microcystis aeruginosa* with Ma-LEP, 5x5 µm.

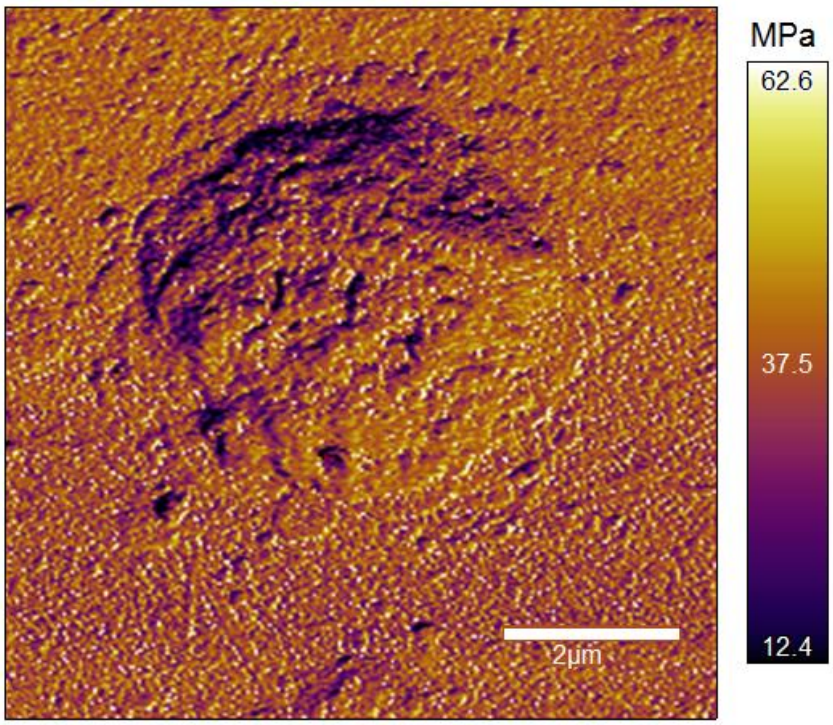

Figure A 27: 1 month incubation of *Microcystis aeruginosa* with Ma-LEP, 10x10 µm.

21.3 Phase Images

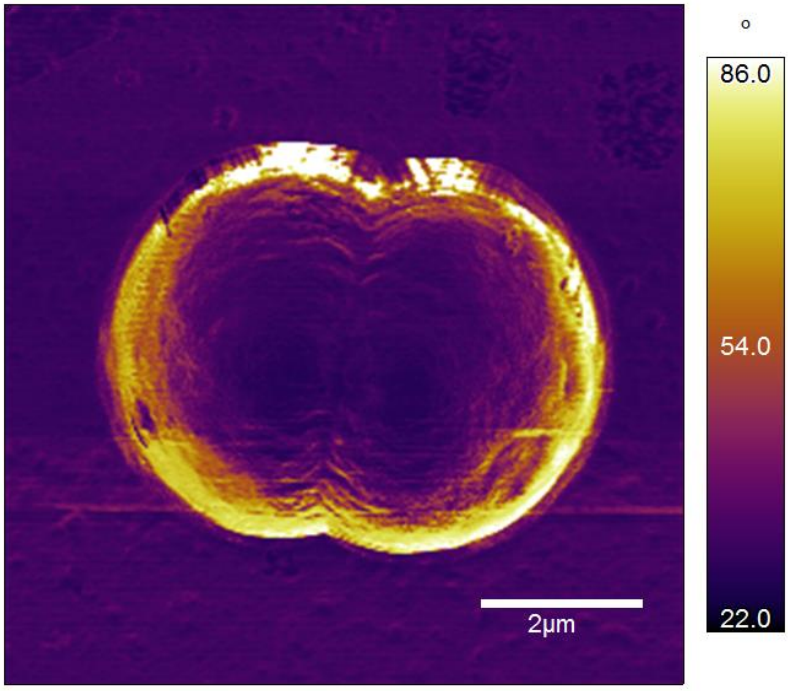

Figure A 28: *Microcystis aeruginosa* (control), 10x10 µm.

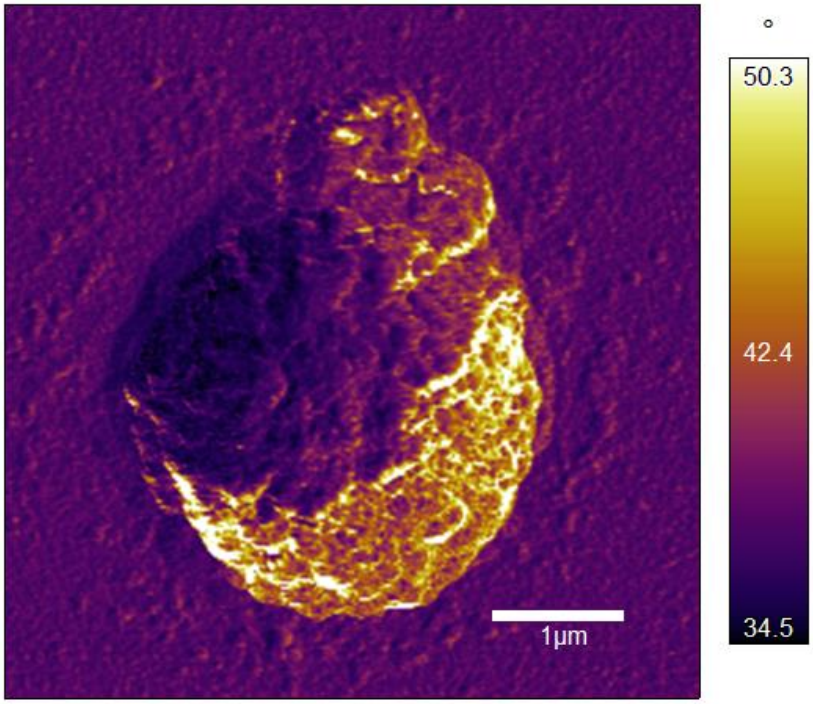

Figure A 29: 4 day incubation of *Microcystis aeruginosa* with Ma-LEP, 5x5 µm.

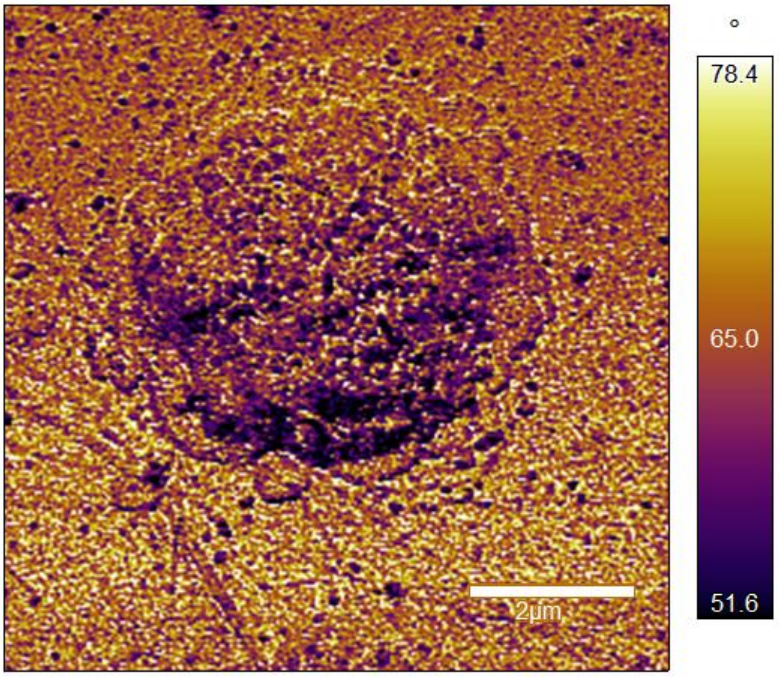

Figure A 30: 1 month incubation of *Microcystis aeruginosa* with Ma-LEP, 10x10 µm.